

Article

Diindolylmethane Derivatives – Potent Agonists of the Immunostimulatory Orphan G Protein-Coupled Receptor GPR84

Thanigaimalai Pillaiyar, Meryem Köse, Katharina Sylvester, Heike Weighardt, Dominik Thimm, Gleice Borges, Irmgard Förster, Ivar von Kügelgen, and Christa E Müller

J. Med. Chem., **Just Accepted Manuscript** • DOI: 10.1021/acs.jmedchem.6b01593 • Publication Date (Web): 13 Apr 2017

Downloaded from <http://pubs.acs.org> on April 13, 2017

Just Accepted

“Just Accepted” manuscripts have been peer-reviewed and accepted for publication. They are posted online prior to technical editing, formatting for publication and author proofing. The American Chemical Society provides “Just Accepted” as a free service to the research community to expedite the dissemination of scientific material as soon as possible after acceptance. “Just Accepted” manuscripts appear in full in PDF format accompanied by an HTML abstract. “Just Accepted” manuscripts have been fully peer reviewed, but should not be considered the official version of record. They are accessible to all readers and citable by the Digital Object Identifier (DOI®). “Just Accepted” is an optional service offered to authors. Therefore, the “Just Accepted” Web site may not include all articles that will be published in the journal. After a manuscript is technically edited and formatted, it will be removed from the “Just Accepted” Web site and published as an ASAP article. Note that technical editing may introduce minor changes to the manuscript text and/or graphics which could affect content, and all legal disclaimers and ethical guidelines that apply to the journal pertain. ACS cannot be held responsible for errors or consequences arising from the use of information contained in these “Just Accepted” manuscripts.



ACS Publications

Diindolylmethane Derivatives – Potent Agonists of the Immunostimulatory Orphan G Protein-Coupled Receptor GPR84

*Thanigaimalai Pillaiyar^{1‡}, Meryem Köse^{1‡}, Katharina Sylvester¹, Heike Weighardt², Dominik Thimm¹,
Gleice Borges¹, Irmgard Förster², Ivar von Kügelgen³ and Christa E. Müller^{1*}*

¹PharmaCenter Bonn, Pharmaceutical Institute, Pharmaceutical Chemistry I, University of Bonn, An der
Immenburg 4, D-53121 Bonn, Germany

²Life and Medical Sciences (LIMES) Institute, Immunology and Environment, University of Bonn,
Carl-Troll-Straße 31, 53115 Bonn, Germany

³Department of Pharmacology and Toxicology, University of Bonn, 53105 Bonn, Germany

[‡]*Authors contributed equally*

^{*}*Corresponding author*

1 KEYWORDS: Agonist, β -Arrestin, Biased Signalling, Diindolylmethane, Free fatty acid receptor, G
2
3 protein-coupled receptors, GPR84, GPR40, GPR120, Orphan receptor, Synthesis, Structure-activity
4
5 relationships
6
7
8
9
10

11 ABSTRACT: The G_i protein-coupled receptor GPR84, which is activated by (hydroxy)fatty acids, is
12
13 highly expressed on immune cells. Recently 3,3'-diindolylmethane was identified as a heterocyclic,
14
15 non-lipid-like GPR84 agonist. We synthesized a broad range of diindolylmethane derivatives by
16
17 condensation of indoles with formaldehyde in water under microwave irradiation. The products were
18
19 evaluated at the human GPR84 in cAMP and β -arrestin assays. Structure-activity relationships (SARs)
20
21 were steep. 3,3'-Diindolylmethanes bearing small lipophilic residues at the 5- and/or 7-position of the
22
23 indole rings displayed the highest activity in cAMP assays, the most potent agonists being di-(5-fluoro-
24
25 1*H*-indole-3-yl)methane (**38**, PSB-15160, EC_{50} 80.0 nM) and di-(5,7-difluoro-1*H*-indole-3-yl)methane
26
27 (**57**, PSB-16671, EC_{50} 41.3 nM). In β -arrestin assays SARs were different indicating biased agonism.
28
29 The new compounds were selective versus related fatty acid receptors and the arylhydrocarbon receptor.
30
31 Selected compounds were further investigated and found to display an ago-allosteric mechanism of
32
33 action and increased stability in comparison to the lead structure.
34
35
36
37
38
39
40
41
42
43
44
45
46
47
48
49
50
51
52
53
54
55
56
57
58
59
60

1
2
3
4
5
6
7
8
9
10
11
12
13
14
15
16
17
18
19
20
21
22
23
24
25
26
27
28
29
30
31
32
33
34
35
36
37
38
39
40
41
42
43
44
45
46
47
48
49
50
51
52
53
54
55
56
57
58
59
60

INTRODUCTION

G protein-coupled receptors (GPCRs) constitute the largest known eukaryotic family of integral membrane proteins with more than 800 human genes that encode for GPCRs. It has been estimated that about one third of all modern drugs are targeting members of this receptor family.¹ Approximately 50 % are non-olfactory receptors and about 100 of these are poorly characterized orphan receptors whose natural ligand and physiological functions are still unknown or unconfirmed.² These orphan receptors are, nevertheless, expected to play important (patho)physiological roles. In the last decade an increasing number of GPCRs has been de-orphanized and it was found that free fatty acids (FFAs) act as ligands for several GPCRs, *i.e.*, GPR40, GPR41, GPR43, GPR120 and GPR84.³⁻⁸ FFAR1 (GPR40), a receptor for long chain free fatty acids, enhances insulin secretion in pancreatic β -cells, among other functions.^{3,6} FFAR2 (GPR43) and FFAR3 (GPR41) are stimulated by short chain fatty acids and are involved in energy regulation in adipocytes.^{4,7} FFAR4 (GPR120) is a receptor for long chain free fatty acids mediating glucagon like peptide-1 secretion.⁵ GPR84 is an exceptional fatty acid-activated receptor which is predominantly present on immune cells.^{9,10} In the periphery, GPR84 is mainly expressed in bone marrow, spleen, lung, and peripheral blood leukocytes. In the CNS, GPR84 expression is restricted to microglia. In addition, GPR84 is expressed in adipose tissues.^{10,11} Table 1 provides a summary of the fatty acid receptors, their coupling and important functions.^{3,4,6,12-14}

Table 1. G protein-coupled fatty acid receptors, their ligands, coupling and physiological functions

Receptor	G protein coupling	Important physiological function	Potent agonists (fatty acids)
FFAR1 (GPR40)	G _{q/11}	Glucose-dependent insulin release, inhibition of osteoclastogenesis ^{15,16} and regulation of taste preference for fatty acids ¹⁷	Long chain, C12-C18
FFAR2 (GPR43)	G _{q/11} , G _{i/o}	Immune function, hematopoiesis, mast cell activity, and adipogenesis. ¹⁸	Short chain, C3=C4=C2
FFAR3 (GPR41)	G _{i/o}	Pancreatic peptide YY (PYY) secretion and glucagon-like peptide 1 (GLP-1) secretion ¹⁹	Short chain, C3=C4>>C2
FFAR4 (GPR120)	G _{q/11}	GLP-1 secretion ⁵	Long chain, C12-C16
GPR84	G _{i/o}	Immunostimulation, ⁹ proinflammatory, ²⁴ defense against pathogens ¹⁰	Medium chain, C9-C14

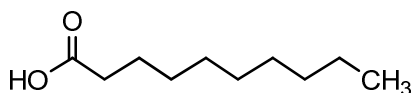
GPR84 was discovered by sequence tag data mining and cloned from a cDNA library prepared from human peripheral blood neutrophils.^{20,21} The human and mouse GPR84 genes encode for a protein of 396 amino acids in length with 85 % identity.²⁰ GPR84 couples primarily to a pertussis toxin (PTX)-sensitive G_{i/o} pathway in response to FFAs, including hydroxylated FFAs, of medium carbon chain length (C9-C14, MCFA).⁹ MCFAs, such as decanoic acid (capric acid), undecanoic acid, and dodecanoic acid (lauric acid) were shown to act through GPR84 in RAW264.7 cells, a murine macrophage-like cell line, amplifying the stimulation of lipopolysaccharide (LPS)-induced interleukin-12B (IL12B) production.^{9,22} The pro-inflammatory cytokine IL-12 plays a pivotal role in promoting cell-mediated immunity to eradicate pathogens by inducing and maintaining T helper 1 (Th1) responses and inhibiting T helper 2 (Th2) response, which plays an important role in antibody-mediated immunity. The expression of GPR84 in the peripheral immune system and in microglia suggests a role in the regulation of (neuro)inflammatory processes.¹⁰ Recent evidence showed that GPR84 deficiency decreased the proliferation of leukemia cells and has therefore been proposed for the treatment of acute

myeloid leukemia.²³ The expression of GPR84 in adipose tissues may indicate that the receptor plays a role in obesity.²⁴ GPR84 may be a promising drug target for a variety of inflammatory diseases including Alzheimer's disease,²⁵ neuropathic pain,²⁶ reflux esophagitis,²⁷ and inflammatory bowel disease.²⁸

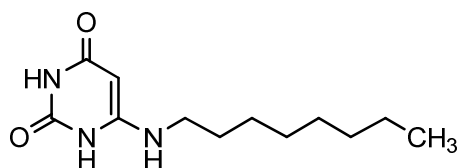
MCFAs are only weakly potent activators of GPR84. Moreover, these putative endogenous ligands of GPR84, including saturated fatty acids ranging in chain length from C9 to C14, also activate the free fatty acid (FFA) receptors FFAR1 (GPR40) and FFAR4 (GPR120).^{6,29,30} Suzuki *et al.* reported that 2-hydroxy- and 3-hydroxy-fatty acids were more potent GPR84 agonists than non-hydroxylated fatty acids. In the same study, 6-*n*-octylaminouracil (6-OAU, Figure 1), which displays a lipid-mimetic structure, was reported as a synthetic agonist of human GPR84 with an EC₅₀ value of 512 nM determined in [³⁵S]GTPγS binding assays.^{13,29,31} More recently, the structurally related 2-(hexylthio)pyrimidine-4,6-diol (Figure 1) and its derivatives^{32,33} were identified as GPR84 agonists. In addition, the natural product embelin (embelic acid, 3-undecyl-2,5-dihydroxy-1,4-benzoquinone, Figure 1) has also been reported to be a GPR84 agonist with moderate potency.³⁴ Embelin is a secondary metabolite originally isolated from the plant *Embelia ribes* (*Primulaceae*), which was reported to have anthelmintic, antifertility, antitumor, anti-apoptotic, antimicrobial, analgesic, and anti-inflammatory activity.³⁵⁻³⁷ Besides GPR84 activation, embelin has several other activities including inhibition of X-linked inhibitor of apoptosis protein (XIAP, IC₅₀ 4.1 μM),³⁸ activation of caspase 9,³⁸ and anti-oxidant properties.³⁹

Another natural product-derived GPR84 agonist, 3,3'-diindolylmethane (**1**, Figure 1) was discovered,⁴⁰ which possibly acts *via* an allosteric binding site since its structure does not resemble fatty acids and is not lipid-like.⁴¹ **1** is the major metabolite of indole-3-carbinol which is a break-down product of glucobrassicin, a glucosinolate that is present in high concentrations in some vegetables such as broccoli.⁴² The compound was previously reported to activate the arylhydrocarbon receptor (AhR), a ligand-activated transcription factor associated with gastric carcinogenesis,⁴³ as well as estrogen

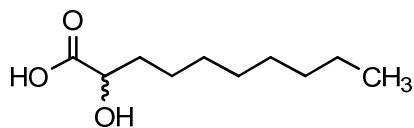
receptors⁴⁴ at concentrations of around 10 μ M and higher. **1** Showed anti-obesity effects in mice.⁴⁵ and displayed anti-cancer activity *in vitro* and *in vivo*.⁴⁶



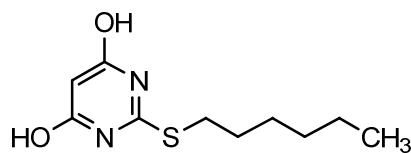
Decanoic acid



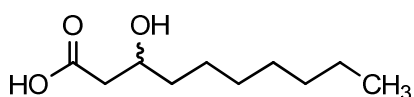
6-Octylaminouracil (6-OAU)



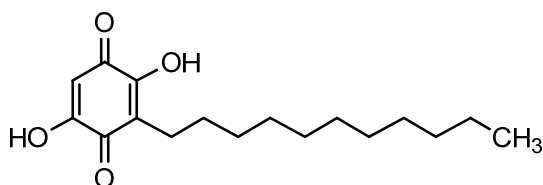
2-Hydroxy-decanoic acid



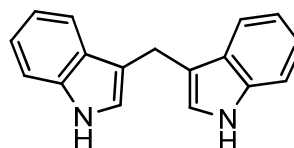
2-Hexylthiopyrimidine-4,6-diol



3-Hydroxy-decanoic acid



Embelin



3,3'-Diindolylmethane (DIM, 1)

Figure 1. Selected GPR84 agonists

While most GPR84 agonists contain long alkyl chains and are thus highly lipophilic, **1** is a small heterocyclic molecule consisting of indole rings, which are found in many perorally applied drug molecules.⁴⁷⁻⁴⁹ In the present study, we therefore selected **1** as a lead molecule and studied its structure-activity relationships (SARs) with the goal to improve its potency. The synthesized compounds were evaluated at the human GPR84 in cAMP accumulation as well as β -arrestin recruitment assays.

RESULTS AND DISCUSSION

Compound design

In order to explore the SARs of diindolylmethane derivatives at GPR84, the following modifications were targeted (Figure 2): (A) substitution of the indole rings in various positions including symmetrical and unsymmetrical substitution patterns, (B) mono-substitution of the 3,3'-methylene linker (C10) by alkyl and aryl residues, (C) replacement of the 3,3'-methylene linker (CH₂) by a carbonyl group, (D) oxidation of the diindolylmethane ring system and (E) subsequent partial reduction yielding compounds E.

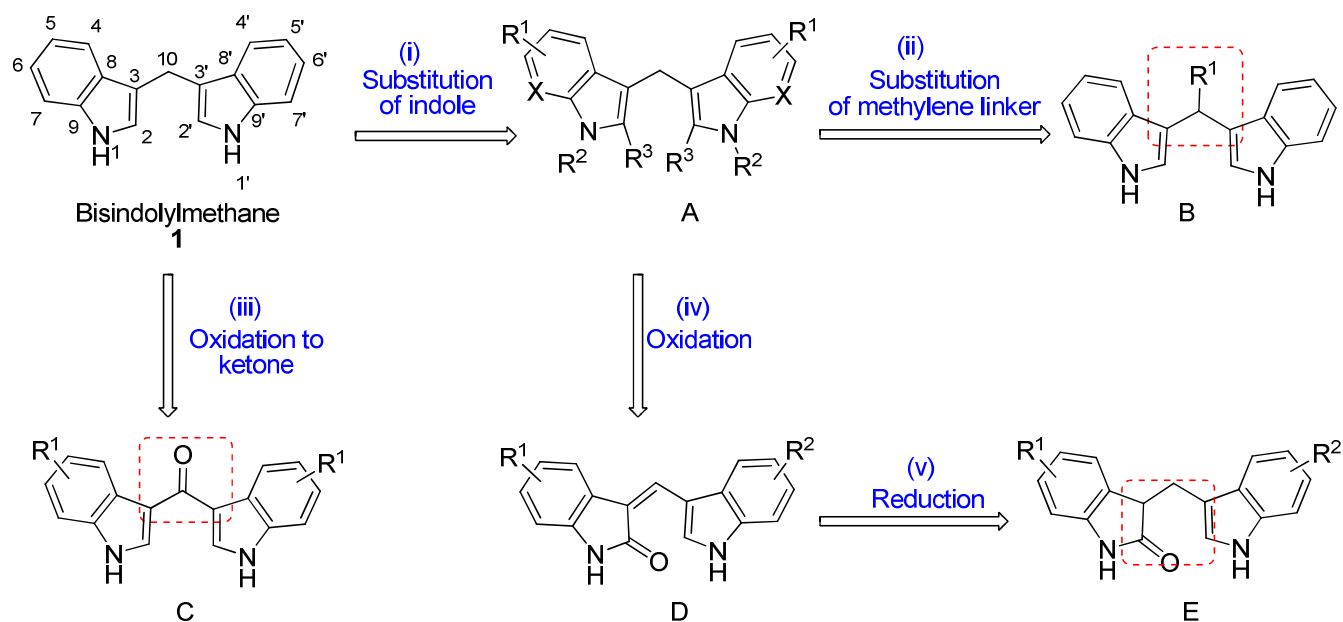


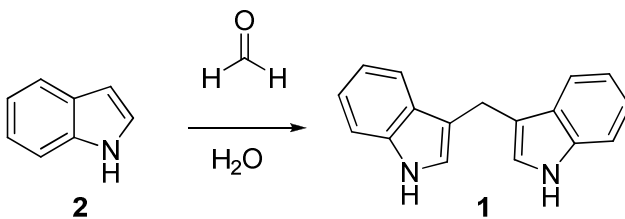
Figure 2. Modifications of 3,3'-diindolylmethane (1)

Chemistry

It is well known that indoles react with aliphatic or aromatic aldehydes and ketones to produce azafulvenium salts; these can undergo further addition with a second indole molecule to afford diindolylmethanes. A number of synthetic methods for the preparation of 3,3'-diindolylmethanes have been reported in the literature using protic acid (e.g. HCl),⁵⁰⁻⁵² Lewis acids (e.g. AlCl₃, BF₃, I₂),^{53,54} or different lanthanide triflates or chlorides.⁵⁵⁻⁵⁸ Recently, benzoic acid⁵⁹ in water, sodium dodecylsulfate (SDS)⁶⁰ as a surfactant in water, oxalic acid and *N*-acetyl-*N,N,N*-trimethylammonium bromide (CTAB)

1 in water,⁶¹ metal triflate in ionic liquid,⁵⁷ in ionic liquids with or without Fe(III) salts^{62,63} were reported
2 to provide efficient conditions for the transformation of indoles to diindolylmethanes. However, there
3 are still a number of drawbacks in the available catalytic systems including the requirement of
4 large^{55,64} or stoichiometric amounts of catalysts,⁶⁵ long reaction times^{55,59,64} and low yields.⁶⁶ Organic
5 reactions in water as a reaction medium offer advantages, including low cost, safe handling and
6 environment-compatibility. There are few reports on the synthesis of diindolylmethanes in water *via* the
7 condensation of indole with aliphatic or aromatic aldehydes.^{59,60} This led us to attempt the reaction of
8 indole with various aldehydes in aqueous media under microwave irradiation. In our initial attempt, the
9 reaction of indole (**2**, 10 mmol) with formaldehyde (37 %, 5 mmol) in water at 100 °C for 5 minutes was
10 selected as a model reaction (entry 1, Table 2). The desired product **1** was isolated in reasonable
11 quantity (43 %) without a catalyst. In order to improve the yield, reaction time, temperature and catalyst
12 were optimized (Table 2). As shown in entries 2–4, the yield was gradually improved by increasing the
13 reaction time, and the best result was obtained for reactions at 100 °C for 20 min (entry 4, 98 % yield).
14 The reaction temperature is one of the most important criteria as the reduction of the temperature from
15 100 °C to 75 or 50 °C in a 30 min reaction resulted in low yield (entry 5 and 6). The reaction was also
16 studied in the presence of acids as catalysts, concd. H₂SO₄ or CH₃COOH, at 100 °C for 30 min;
17 however, these conditions resulted in poor yields (20 % for entry 7 and 30 % for entry 8, Table 2).
18
19
20
21
22
23
24
25
26
27
28
29
30
31
32
33
34
35
36
37
38
39
40
41
42
43
44
45
46
47
48
49
50
51
52
53
54
55
56
57
58
59
60

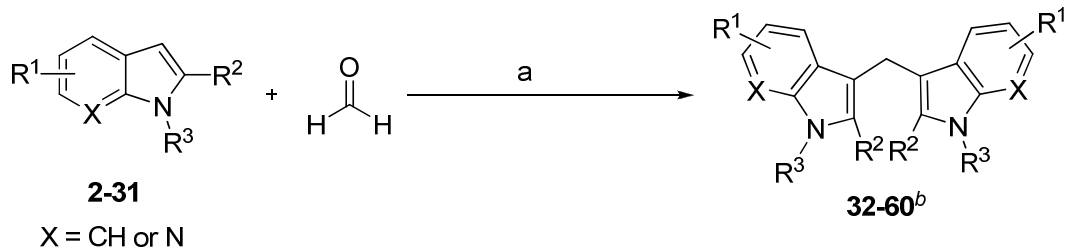
Table 2. Microwave-assisted synthesis of 3,3'-diindolylmethane in water under different conditions



Entry	Catalyst	Temp (°C)	Time (min)	Power (W)	Yield (%)
1	-	100	5	105	43
2	-	100	10	105	84
3	-	100	15	105	91
4	-	100	20	105	98
5	-	75	30	75	42
6	-	50	30	75	28
7	concd. H ₂ SO ₄	100	20-30	105	20
8	CH ₃ CO ₂ H	100	20-30	105	30

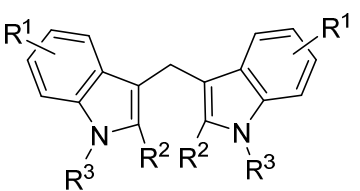
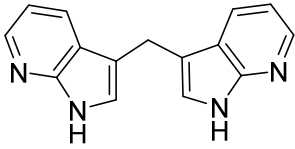
The optimized conditions were subsequently used for the synthesis of a series of diindolylmethane derivatives (Scheme 1). The desired products **32-60** were obtained from the starting indoles **2-31** in very good to excellent yields (84-98 % isolated). Detailed reaction conditions and purities of the products (**32-60**) are summarized in Table 3. It should be noted that the microwave-assisted reactions were completed within only 20-30 min for most of the derivatives.

Scheme 1. Synthesis of 3,3'-diindolylmethane derivatives **32-60**^a



^aReagents and conditions: (a) H₂O, 100 °C, microwave, 20–180 min, yield 45–98 %. ^b For R¹, R² and R³ see Table 3.

Table 3. Reaction times, yields, melting points and purities of 3,3'-diindolylmethane derivatives

<div style="display: flex; justify-content: space-around; align-items: center;"> <div style="text-align: center;">  <p>32-59</p> </div> <div style="text-align: center;">  <p>60</p> </div> </div>					
Compd.	R ¹	R ²	R ³	Time (min)	Yield (%)
1 ⁶⁰	H	H	H	20	98
32 ⁶⁷	4-CH ₃	H	H	25	93
33 ⁶⁸	4-OCH ₃	H	H	25	87
34	4-F	H	H	25	82
35	4-Cl	H	H	25	86
36 ⁶⁷	5-CH ₃	H	H	25	91
37 ⁶⁷	5-OCH ₃	H	H	25	89
38 ⁶⁷	5-F	H	H	30	90
39 ⁶⁷	5-Cl	H	H	20	92
40 ⁶⁷	5-Br	H	H	25	87
41 ⁶⁹	5-CN	H	H	29	92
42 ⁶⁹	5-NO ₂	H	H	35	90
43	5-COOMe	H	H	25	84

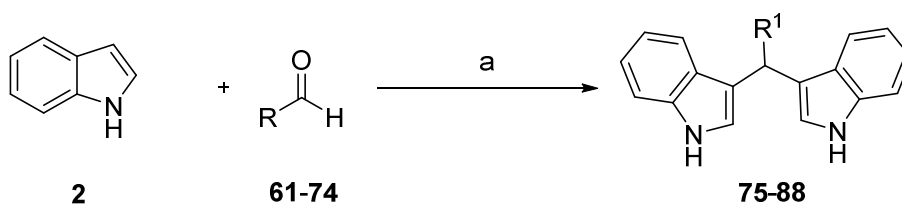
1	44	5-CHO	H	H	25	85
2						
3						
4	45	5-COOH	H	H	25	79
5						
6						
7	46	5-OCH ₂ Ph	H	H	35	75
8						
9						
10	47 ⁶⁸	6-CH ₃	H	H	25	88
11						
12						
13	48 ⁶⁸	6-OCH ₃	H	H	25	82
14						
15						
16	49 ⁶⁸	6-F	H	H	30	87
17						
18						
19						
20	50 ⁶⁸	6-Cl	H	H	25	90
21						
22						
23	51	7-OCH ₃	H	H	25	93
24						
25						
26	52	7-F	H	H	25	85
27						
28						
29	53	4-Cl, 6-Cl	H	H	30	83
30						
31						
32	54	5-F, 6-Cl	H	H	30	76
33						
34						
35	55	4-F, 5-F	H	H	20	87
36						
37						
38	56	5-F, 6-F	H	H	20	83
39						
40						
41	57	5-F, 7-F	H	H	30	80
42						
43						
44	58 ⁷⁰	H	H	CH ₃	25	89
45						
46	59 ⁶⁸	CH ₃	CH ₃	H	25	82
47						
48						
49	60 ⁶⁸	see structure above			25	82
50						
51						
52						
53						

Surfactants can play an important role as emulsifiers in water-mediated organic reactions.^{59,60,71} In order to avoid solubility problems, we used sodium dodecyl sulfate (SDS) in our next optimization step

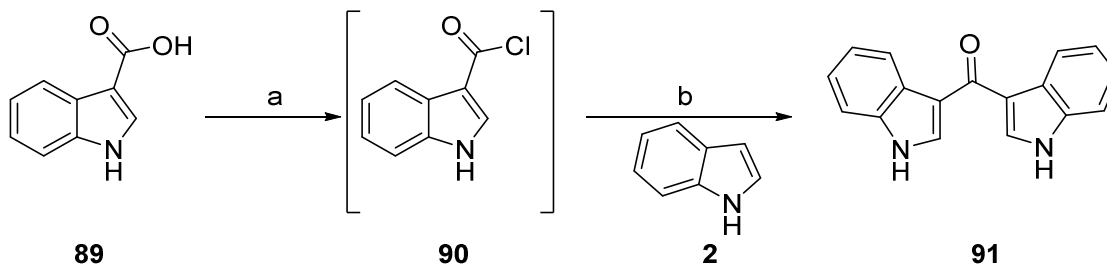
1 reacting indoles with various aliphatic and aromatic aldehydes under microwave irradiation in water.
2
3 Indole **2** was treated with the appropriate aldehyde in the presence of 10 % SDS in water (5 mL), and
4
5 the resulting white turbid mixture was irradiated in a microwave oven at 100 °C for 30-40 min (Scheme
6
7 2A). As shown in Table 4, both, aliphatic (**61-66**) and aromatic aldehydes (**67-74**), afforded good yields
8
9 of the corresponding products (**75-88**).^{60,71-76} Diindolylmethanone **92** was synthesized using a published
10
11 procedure as indicated in Scheme 2B.⁷⁷ Indole-3-carboxylic acid (**89**) was converted to the
12
13 corresponding acid chloride **90** by reaction with thionyl chloride in dichloromethane at 45 °C for 1 h.
14
15 The resulting acid chloride was subsequently treated with indole (**2**) in the presence of zirconium(IV)
16
17 chloride in dichloroethane at room temperature for 4 h to produce the desired product **91**.
18
19
20
21
22
23
24
25
26
27
28
29
30
31
32
33
34
35
36
37
38
39
40
41
42
43
44
45
46
47
48
49
50
51
52
53
54
55
56
57
58
59
60

Scheme 2. Synthesis of diindolylmethane derivatives **75-88**^a and **91**^b

A)

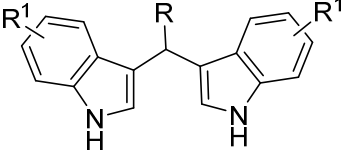
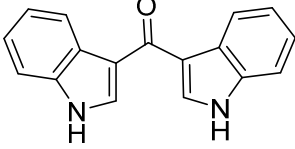
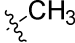
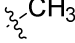


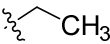
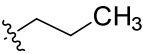
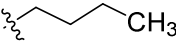
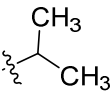
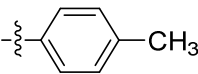
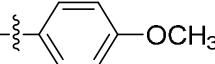
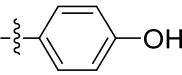
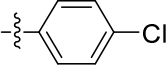
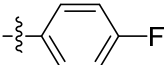
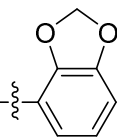
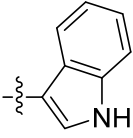
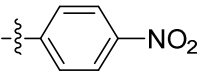
B)



^aReagents and conditions: (a) sodium dodecyl sulfate (SDS), H₂O, 95–100 °C, microwave (MW), 30-40 min, yield 72–95 %. For R see Table 5; ^b(a) SOCl₂, dichloroethane (DCE), 40 °C, 1 h; b) ZrCl₄, DCE, 0 °C to rt, 4 h, 69 %.

Table 4. Reaction times, yields, melting points and purities of products **75-88** and **91**

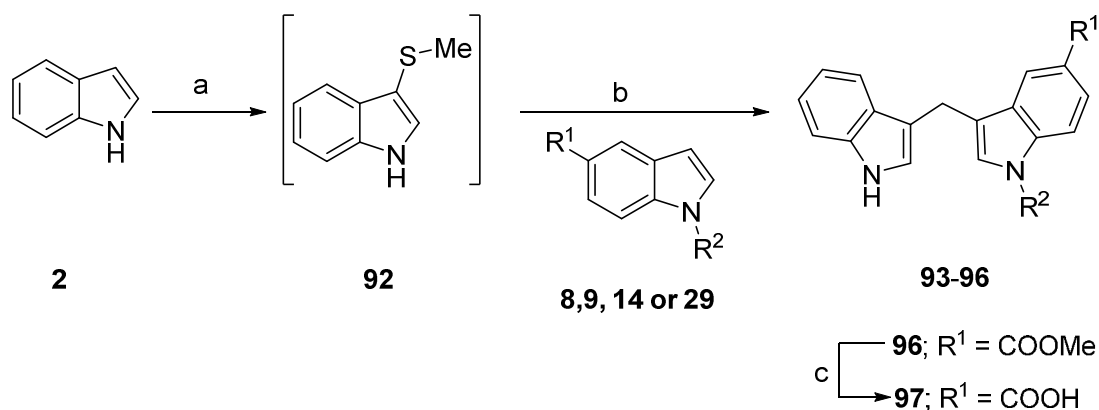
				
Compd.	R	R ¹	Reaction time (min)	Yield (%) (lit. yield)
75 ⁷²		H	30	89
76		4-F	30	83

77		H	30	80
78 ⁷³		H	30	84 (73)
79 ⁷⁴		H	30	89 (62)
80 ⁷⁵		H	35	72 (21)
81 ⁵²		H	40	85 (65)
82 ⁵²		H	40	95 (80)
83		H	40	93
84 ⁵²		H	40	87 (55)
85		H	40	80
86		H	40	91
87 ⁷⁶		H	40	94 (89)
88 ⁵²		H	40	90 (60)

1
2
3
4
5
6
7
8
9
10
11
12
13
14
15
16
17
18
19
20
21
22
23
24
25
26
27
28
29
30
31
32
33
34
35
36
37
38
39
40
41
42
43
44
45
46
47
48
49
50
51
52
53
54
55
56
57
58
59
60

91 ⁷⁷	See structure above	40	69
-------------------------	---------------------	----	----

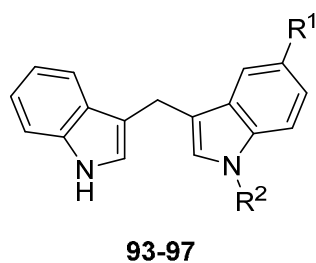
Unsymmetrical 3,3'-diindolylmethanes were synthesized through an intermolecular Pummerer reaction using indole as a nucleophile.⁷⁸ As shown in Scheme 3, indole was treated with dimethyl sulfoxide (DMSO) and trifluoroacetic acid anhydride in 1,4-dioxane at 0 °C, and the mixture was heated at 80 °C for 30 min to obtain intermediate **92**, which was subsequently converted to the unsymmetrical 3,3'-diindolylmethanes **93–97** by heating it with substituted indole (**8**, **9**, **14** or **29**) and copper acetate for 2 h. Product **97** was obtained in an excellent yield of 99 % after hydrolysis of the dimethyl ester **96**, which was achieved by treatment with 2-*N* sodium hydroxide in ethanol under reflux for 2 h. Yields, melting points and purities of synthesized derivatives are collected in Table 5.

Scheme 3. Synthesis of unsymmetrical 3,3'-diindolylmethanes **93-98**^a

^aReagents and conditions: (a) DMSO, trifluoroacetic anhydride (TFAA), dioxane, 0 °C then 80 °C, 30 min; (b) Cu(OAc)₂, dioxane, 80 °C, 1 h, yield 35–47%; c) 2 N NaOH, ethanol, 100 °C, 1 h, yield 99%.

For R¹, R² see Table 5.

Table 5. Yields, melting points and purities of synthesized unsymmetrically substituted 3,3'-diindolylmethanes (**93–97**)

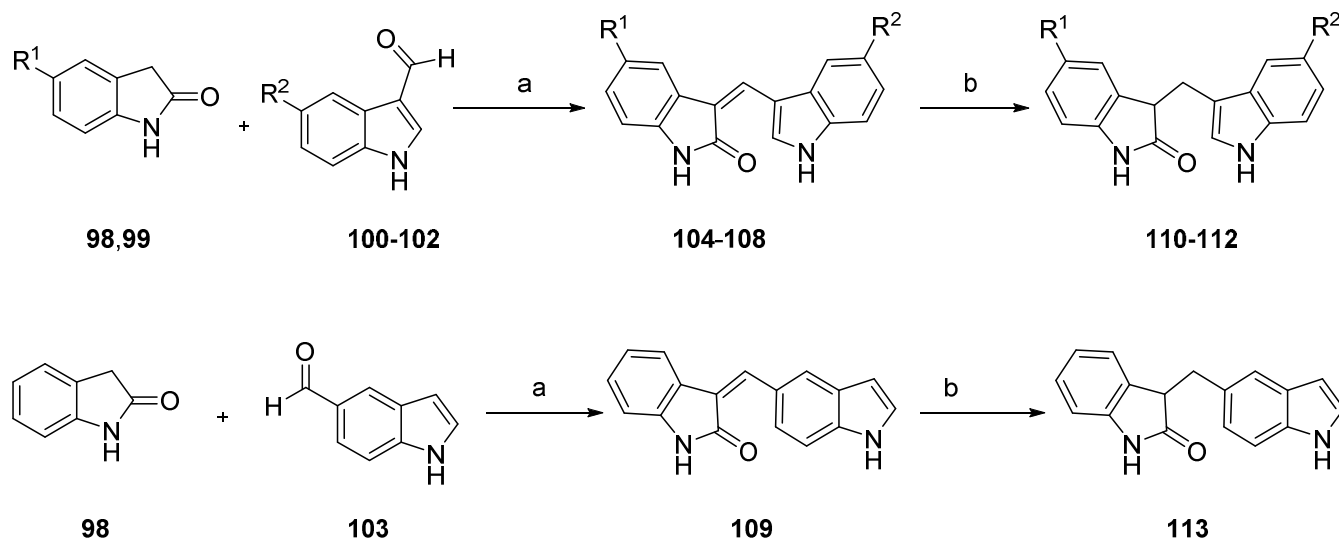


Compd.	R ¹	R ²	Yield (%)
93	H	CH ₃	40
94	OCH ₃	H	47
95	F	H	41
96	CO ₂ CH ₃	H	35
97	CO ₂ H	H	99

2-Oxoindole derivatives were synthesized as illustrated in Scheme 4. 2-Oxoindole derivative **98** or **99** was reacted with the appropriate aldehyde (**100-103**) in absolute ethanol in the presence of piperidine at 65 °C for 2 h to produce α,β -unsaturated indole-2-one derivatives **104-109**.⁷⁹⁻⁸³ These products were reduced in the presence of sodium borohydride at 65 °C for 2 h to yield the corresponding saturated indole-2-one derivatives **110-113**.⁷⁹

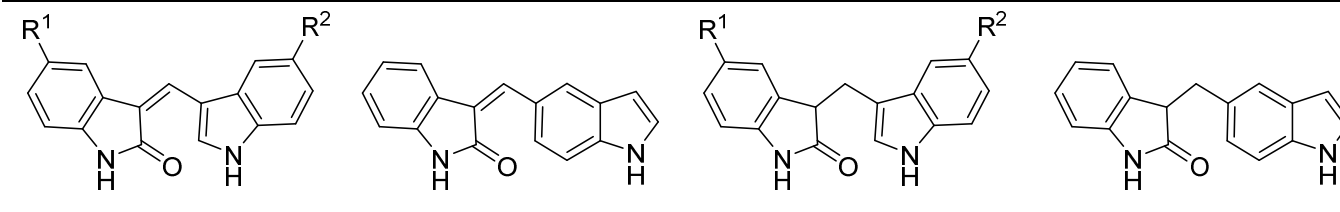
The structures of the synthesized compounds were confirmed by ¹H, ¹³C, and/or ¹³C attached protein test (¹³C_{apt}) NMR spectroscopy, a common experiment to assign C-H multiplicities in ¹³C NMR spectra. In addition, HPLC analysis coupled to electrospray ionization mass spectrometry (LC/ESI-MS) was performed, which was also used to determine the purity of the compounds.

Scheme 4: Synthesis of unsaturated and saturated 2-oxoindole derivatives **104-109** and **110-113**^a



^aReagents and condition: (a) piperidine, ethanol, 65 °C, 2 h, yield 69–80%; (b) NaBH₄, ethanol, 65 °C, 2 h, yield 73–95%. For R^1 , R^2 see Table 6.

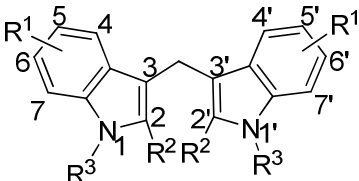
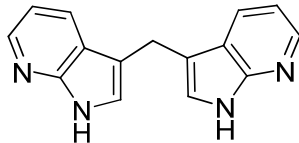
Table 6. Yields, melting points and purities of synthesized 2-oxoindole derivatives **104-113**

			
104-108	109	110-112	113
Compd.	R ¹	R ²	Yield (%)
104 ⁸⁰	H	H	76
105	H	F	69
106 ⁷³	H	OCH ₃	73
107 ⁸¹	F	F	85
108	F	OCH ₃	80
109 ⁸³	See structure above		73
110 ⁸²	H	OCH ₃	89
111	F	F	96
112	F	OCH ₃	91
113	See structure above		95

Pharmacological evaluation

All compounds were initially investigated in cAMP accumulation assays at a concentration of 10 μ M for their potency to inhibit forskolin (10 μ M) induced cAMP accumulation in Chinese hamster ovary (CHO) cells stably expressing the G_i protein-coupled human GPR84. For compounds leading to more than 50 % inhibition of cAMP accumulation, full concentration-response curves were determined and EC₅₀ values were calculated (see Table 7 and 8). In order to determine the compounds' efficacy, their maximal effects were compared to the maximal signal induced by decanoic acid (100 μ M; EC₅₀ 7.42 μ M). Compounds that did not show agonistic activity were tested for their potency to antagonize receptor activation by decanoic acid (20 μ M) at a concentration of 10 μ M. To exclude GPR84-independent effects, the most potent compounds were additionally investigated in the parent non-GPR84-transfected CHO cell line. Selected compounds were further investigated in GPR84-dependent β -arrestin recruitment assays using the β -galactosidase fragment complementation technology (Pathhunter, DiscoverX)^{84,85} (see Table 7 and 8). We additionally confirmed the allosteric interaction of diindolylmethane and its optimized derivative **57** with GPR84 in cAMP accumulation assays applying different combinations of the orthosteric agonist decanoic acid and diindolylmethanes. To investigate GPR84 selectivity, potent agonists were evaluated at those human free fatty acid receptor subtypes that show overlapping agonist specificity with GPR84 and are also activated by dodecanoic acid, namely FFAR1 and FFAR4 (see Table S2 and S3). The G_q protein-coupled human FFAR1 was retrovirally expressed in 1321N1 astrocytoma cells and calcium mobilization assays were performed. The human FFAR4 was expressed in a CHO cell line suitable to perform β -arrestin recruitment assays using the β -galactosidase complementation assay technology. All compounds were tested for agonistic as well as antagonistic activity at FFAR1 and FFAR4 in a final concentration of 10 μ M. Selected diindolylmethane derivatives were further evaluated for activation of the arylhydrocarbon receptor, the most prominent target of lead compound **1**.

Table 7. Potency of symmetrical 3,3'-diindolylmethane derivatives **32–60** as agonists at the human GPR84 determined in cAMP accumulation and β -arrestin recruitment assays

<div>  <p>32-59</p> </div> <div>  <p>60</p> </div>					
Compd.	R ¹	R ²	R ³	human GPR84	
				cAMP assay ^a	β-arrestin assay
				EC ₅₀ ± SEM (μM) (or percent receptor activation at 10 μM) [<i>efficacy</i>] ^b	EC ₅₀ ± SEM (μM) (or percent receptor activation at 10 μM) [<i>efficacy</i>] ^c
Decanoic acid				7.42 ± 0.40 [<i>100</i> %] [*]	6.08 ± 0.36 [92 %] [#]
Embelin				0.795 ± 0.168 [86 %] [§]	0.400 ± 0.142 [<i>100</i> %] [§]
1	H	H	H	0.252 ± 0.088 [125 %]	1.64 ± 0.81 [60 %]
32	4-CH ₃	H	H	0.987 ± 0.235 [112 %]	> 10 (24 ± 8 %)
33	4-OCH ₃	H	H	≥ 10 (47 ± 17 %)	n.d. [*]
34 (PSB-16357)	4-F	H	H	0.328 ± 0.005 [110 %]	1.23 ± 0.03 [108 %]
35	4-Cl	H	H	1.14 ± 0.06 [111 %]	> 10 (25 ± 14 %)
36	5-CH ₃	H	H	≥ 10 (45 ± 9 %)	≥ 10 (49 ± 6 %)
37 (PSB-16105)	5-OCH ₃	H	H	0.369 ± 0.025 [119 %]	1.20 ± 0.80 [103 %]
38 (PSB-15160)	5-F	H	H	0.0800 ± 0.0212 [117 %]	4.33 ± 2.12 [125 %]
39	5-Cl	H	H	4.96 ± 3.08 [86 %]	n.d.
40	5-Br	H	H	3.44 ± 0.29 [106 %]	n.d.
41	5-CN	H	H	≥ 10 (49 %)	n.d.
42	5-NO ₂	H	H	> 10 (31 %)	n.d.
43	5-COOMe	H	H	> 10 (11 %)	n.d.
44	5-CHO	H	H	> 10 (-4 %)	n.d.

1	45	5-COOH	H	H	≥ 10 (28 %)	$\gg 10$ (-5 \pm 6 %)
2	46	5-OCH ₂ Ph	H	H	> 10 (36 %)	n.d.
3						
4	47	6-CH ₃	H	H	> 10 (-22 %)	n.d.
5						
6	48	6-OCH ₃	H	H	> 10 (31 %)	n.d.
7						
8	49 (PSB-	6-F	H	H	0.625 ± 0.070 [89 %]	7.53 ± 2.30 [48 %]
9	16358)					
10						
11	50	6-Cl	H	H	> 10 (4 %)	5.34 ± 1.84 [118 %]
12						
13	51	7-OCH ₃	H	H	> 10 (18 %)	n.d.
14						
15	52 (PSB-	7-F	H	H	0.113 ± 0.047 [129 %]	6.07 ± 3.37 [99 %]
16	16381)					
17						
18	53	4-Cl,6-Cl	H	H	≥ 10 (51 %)	n.d.
19						
20	54	5-F,6-Cl	H	H	10.8 ± 0.50 [83 %]	3.98 ± 0.86 [181 %]
21						
22	55	4-F,5-F	H	H	0.377 ± 0.030 [123 %]	$\gg 10$ (-2 \pm 9 %)
23						
24	56 (PSB-	5-F,6-F	H	H	0.187 ± 0.053 [121 %]	10.3 ± 5.6 [92 %]
25	16586)					
26						
27	57 (PSB-	5-F,7-F	H	H	0.0413 ± 0.0098 [131 %]	5.47 ± 0.13 [385 %]
28	16671)					
29						
30	58	H	H	CH ₃	> 10 (-37 %)	$\gg 10$ (-3 %)
31						
32	59	H	CH ₃	H	≥ 10 (42 %)	> 10 (23 %)
33						
34	60	see structure above	-		> 10 (-12 %)	2.27 ± 0.42 [115 %]

35 *n.d., not determined

36 ^aInhibition of forskolin (10 μ M) induced decrease in cAMP accumulation

37 ^bEfficacy (E_{max}) relative to the max. effect of decanoic acid (100 μ M) (= 100 %)

38 ^cEfficacy (E_{max}) relative to the max. effect of embelin (10 μ M) (= 100 %)

39 ^{*} Literature value: $EC_{50} = 4.5 \pm 0.3 \mu M^9$

40 [#] Literature value: $EC_{50} = 10 \mu M^{84}$

41 [§] Literature value: $EC_{50} = 421 \text{ nM}^{85}$

42 [§] Literature value: $EC_{50} = 12.3 \mu M^{84}$

Structure-activity relationships

cAMP accumulation assays

The lead compound **1** induced an inhibition of forskolin-induced cAMP accumulation in CHO cells transfected with the human G_i-coupled GPR84 displaying an EC₅₀ 252 nM. (see Fig. 4). It was 29-fold

more potent than decanoic acid ($p=0.0021, **$) and showed a higher efficacy (125 %) compared to decanoic acid (set at 100 %) that – in contrast to **1** - did not completely inhibit cAMP formation at the highest concentration used (Fig. 4). We confirmed that **1** had no effect on forskolin-induced cAMP levels in non-transfected CHO cells (see Fig. 4). This clearly proves that the observed effect on cAMP levels was due to GPR84 activation.

When exploring the SARs of diindolylmethane derivatives we initially focused on substitution of the indole rings (Table 7). SAR analysis revealed that many symmetrically substituted indole derivatives were potent GPR84 agonists. However, substitution at several positions of the indole rings resulted in loss of activity, and substitution was only permitted in few positions. These results indicated very steep SARs, clearly not driven by an increase in lipophilicity.

The following substituents were introduced at the 4,4'-positions of the indole rings: 4,4'-dimethyl (**32**), 4,4'-dimethoxy (**33**), 4,4'-difluoro (**34**) and 4,4'-dichloro (**35**). A deleterious effect on activity was observed with these substituents, except for compound **34** (EC_{50} 328 nM) featuring 4,4'-difluoro substitution, which exhibited comparable activity to the lead compound (**1**). Next, substituents were introduced at the 5,5'-positions yielding compounds **36–46**. Among them, the 5,5'-difluoro derivative (**38**: EC_{50} 80.0 nM) showed high activity being 3-fold more potent than the lead compound **1**. 5,5'-Dimethoxy substitution (**37**: EC_{50} 369 nM) conferred moderate potency, whereas 5,5'-dichloro (**39**: EC_{50} 4960 nM) and 5,5'-dibromo derivatives (**40**: EC_{50} 3440 nM) displayed only weak potency. Substitution at the 6,6'-positions (compounds **47–50**) did not improve agonistic potency, and the small 6,6'-difluoro substituents were best tolerated (compound **49**, EC_{50} 625 nM). Based on these results we only prepared two 7,7'-substituted diindolylmethanes with 7,7'-dimethoxy (**51**) and 7,7'-difluoro (**52**) derivatives. Interestingly, compound **52** (EC_{50} 113 nM) was found to be 6-fold more potent than the corresponding 6,6'-difluoro-substituted isomer **49** (EC_{50} 625 nM) ($p=0.0057, **$), and appeared to be slightly more potent than lead compound **1**.

Encouraged by these results our next effort was to introduce multiple halogen substituents with the goal to identify the best combination (compounds **53-57**). Chloro substitution at the 4- and 6- positions (**53**) was not tolerated probably because of the size of the halogen atoms. When we introduced the smaller fluorine atoms, the potency of the resulting compounds (**54-57**) was much higher. A combination of fluorine atoms in the 5- and 7-positions (**57**) was found to be the best combination, and in fact compound **57** (EC_{50} 41.3 nM) was the most potent GPR84 agonist of the present series.

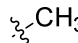
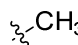
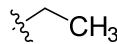
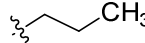
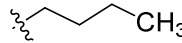
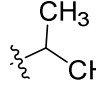
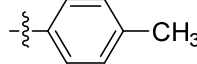
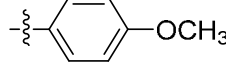
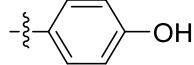
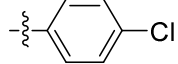
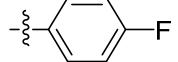
The replacement of the indole NH hydrogen atoms of lead structure **1** by methylation yielding the 1,1'-dimethyl derivative **58** (EC_{50} >10 μ M) or the 1-methyl derivative **59** (EC_{50} \geq 10 μ M, see Table 8) abolished potency of the compound. This confirms that the indole NH functions are very important for interaction with GPR84, presumably by the formation of hydrogen bonds. Substitution of the 2-positions as in the 2,2'-dimethyl derivative **59**, or introduction of a nitrogen atom as in di-(7'-azaindoly)methane (**60**) was not tolerated. These results obtained from substitution and modification of the indole rings clearly indicated that substituents other than fluoro were not well tolerated and in all cases led to a decrease in agonistic potency at GPR84. The rank order of potency for substituents at various positions of the indole rings is as follows: 5,5'-difluoro (**38**: EC_{50} 80.0 nM), 7,7'-difluoro (**52**: EC_{50} 113 nM) > 4,4'-difluoro (**34**: EC_{50} 328 nM, $p=0.0104$, *) \geq 5,5'-dimethoxy (**37**: EC_{50} 369 nM) > 6,6'-difluoro (**49**: EC_{50} 625 nM, $p=0.0262$ *). Only fluoro-substitution in the 7- and particularly in the 5-position improved the potency of the unsubstituted lead structure **1**.

In the next set of experiment, we investigated the effects of mono-substitution at the 5-position of only one of the indole rings (Table 8). The following rank order of potency was observed: 5-fluoro (**95**: EC_{50} 264 nM) > 5-methoxy (**94**: EC_{50} 1890 nM, $p=0.0013$, *) > 5-carboxymethyl ester (**96**: EC_{50} \geq 10 μ M) > 5-carboxylic acid (**97**: EC_{50} \gg 10 μ M). This means that also in the mono-substituted series only small residues were tolerated in the 5-position, and a fluorine atom (compound **95**) was best showing similar potency as the unsubstituted lead structure **1**. The potencies of the mono-substituted derivatives **94** (5-

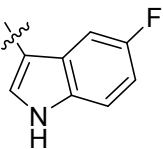
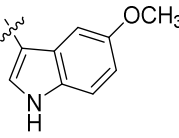
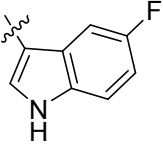
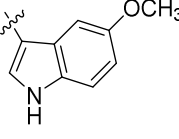
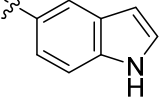
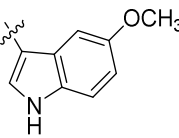
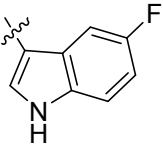
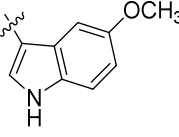
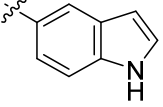
1 fluoro) and **95** (5-methoxy) were reduced when compared to the corresponding di-substituted
2 derivatives **37** ($p=0.0014$, **) and **38** ($p=0.0776$, ns). These results revealed that symmetrical substitution
3 of **1** is superior to mono-substitution yielding unsymmetrical diindolylmethane derivatives (compare
4
5
6
7 **37/94** and **38/95**).
8

9
10
11 We subsequently examined the effects of substitution at the 3,3'-methylene bridge (C-10) of **1** (Table 8).
12
13 A large variety of substituents including methyl (**75-77**), *n*-propyl (**78**), *n*-butyl (**79**), isopropyl (**80**), 4-
14 tolyl (**81**), 4-anisyl (**82**), 4-hydroxyphenyl (**83**), 4-chlorophenyl (**84**), 4-fluorophenyl (**85**), 4-(1,3-
15 benzodioxolyl) (**86**), 3-indolyl (**87**) and 4-nitrophenyl (**88**) were introduced. However, none of the
16 substituents was tolerated at that position, and all compounds were inactive. On the other hand, 3,3'-
17 diindolylmethanone (**91**: EC₅₀ 553 nM), an oxidized derivative of **1**, was found to be almost as potent as
18
19
20
21
22
23
24
25
26 the lead structure **1** (EC₅₀ 252 nM).
27
28
29
30
31
32
33
34
35
36
37
38
39
40
41
42
43
44
45
46
47
48
49
50
51
52
53
54
55
56
57
58
59
60

Table 8. Potency of 3,3'-diindolylmethane derivatives **75-113** as agonists at the human GPR84 determined in cAMP accumulation and β -arrestin recruitment assays

Human GPR84				
Compound	R ¹	R ²	cAMP assay ^a	β-arrestin assay
			EC ₅₀ ± SEM (μM) (or percent receptor activation at 10 μM) [<i>efficacy</i>] ^b	EC ₅₀ ± SEM (μM) (or percent receptor activation at 10 μM) [<i>efficacy</i>] ^c
Structure A: Substitution of the methylene linker (C10)				
75		—	> 10 (-5 %)	> 10 (3 %)
76		4-F	> 10 (5 %)	> 10 (34 %)
77		—	> 10 (-24 %)	2.97 ± 1.03 [67 %]
78		—	> 10 (-24 %)	6.07 ± 0.77 [199 %]
79		—	> 10 (-4 %)	> 10 (-3 %)
80		—	> 10 (16 %)	7.29 ± 0.19 [167 %]
81		—	> 10 (2 %)	> 10 (10 %)
82		—	> 10 (-3 %)	n.d.
83		—	> 10 (7 %)	> 10 (-5 %)
84		—	> 10 (-4 %)	n.d.
85		—	> 10 (8 %)	n.d.

86		—	> 10 (0 %)	> 10 (7 %)
87		—	> 10 (-10 %)	> 10 (10 %)
88		—	> 10 (6 %)	n.d.
Structure B: Diindolylmethanone and unsymmetrically substituted diindolylmethane derivatives				
91 (PSB-16359)		—	0.553 ± 0.141 [104 %]	19.0 ± 8.1 [161 %]
93		—	≥ 10 (43 %)	> 10 (8 %)
94		—	1.89 ± 0.19 [97 %]	6.47 ± 3.20 [110 %]
95 (PSB-16244)		—	0.264 ± 0.075 [115 %]	1.08 ± 0.58 [72 %]
96		—	ca. 10 (57 %)	n.d.
97		—	> 10 (5 %)	n.d.
Structure C: Oxidized products of diindolylmethane derivatives (methene bridged)				
104	H		> 10 (-17 %)	> 10 (-22 %)

105	H		> 10 (-1 %)	n.d.
106	H		> 10 (-10 %)	n.d.
107	5-F		> 10 (5 %)	n.d.
108	5-F		> 10 (7 %)	> 10 (-31 %)
109	H		> 10 (-16 %)	> 10 (-7 %)
Structure D: 2-Oxodihydroindolyl-indolylmethane derivatives				
110	H		> 10 (-21 %)	n.d.
111	5-F		> 10 (16 %)	n.d.
112	5-F		> 10 (-10 %)	n.d.
113	H		> 10 (7 %)	n.d.

^aInhibition of forskolin (10 μM) induced decrease in cAMP accumulation

^bEfficacy (E_{max}) related to the max. effect of decanoic acid (100 μM) (= 100 %)

^cEfficacy (E_{max}) related to the max. effect of embelin (10 μM) (= 100 %)

To obtain deeper insight into the SARs of diindolylmethane derivatives, we altered the hydrogen bonding characteristics of **1** by preparing 2-oxyindoles. To this end we prepared a series of unsaturated (**104–109**) and saturated 2-oxyindole derivatives (**110–113**). However none of these compounds was

found to interact with GPR84 (see Table 8) and this might be due to disruption of the planarity of the molecules.

Figure 3 summarizes the structure-activity relationships of the investigated compounds as agonists of the human GPR84: (i) symmetrical diindolylmethane derivatives show the highest potency, (ii) small substituents like methoxy and fluoro are tolerated at C4, C5, and C7 of the benzene rings, e.g., 4,4'-difluoro- (**34**), 5,5'-dimethoxy- (**37**) and 5-fluoro-diindolylmethane (**95**) show similar potency as the unsubstituted lead structure, while 5,5'-difluoro- (**38**), 7,7'-difluoro- (**52**), and 5,5',7,7'-tetrafluoro-diindolylmethane (**57**) display enhanced agonistic potency; (iii) substitutions or modifications of the methylene linker are not tolerated.

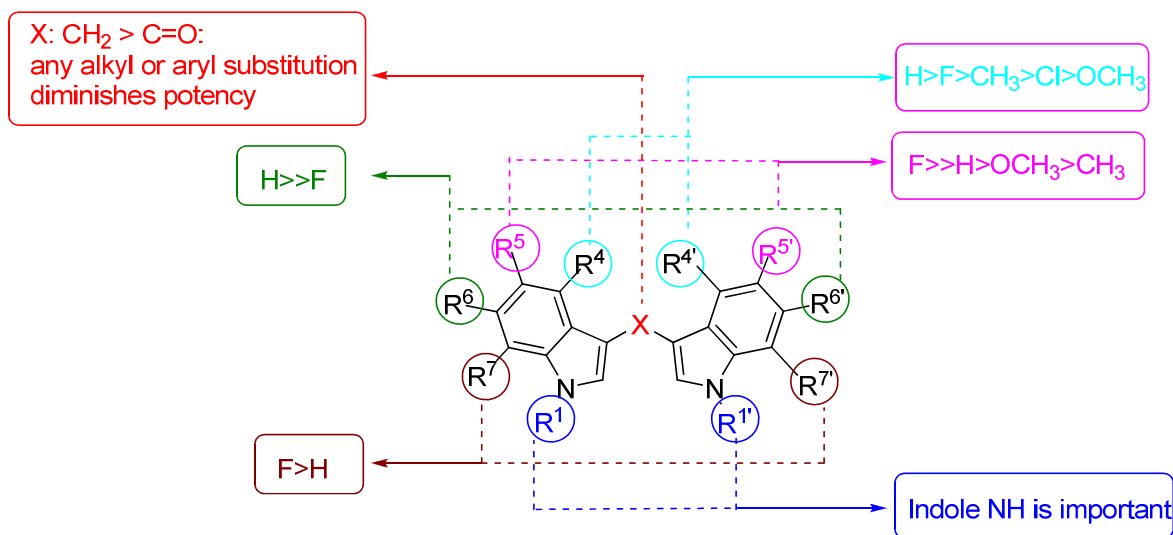


Figure 3: Structure-activity relationships of diindolylmethane derivatives as agonists at human GPR84

Concentration-response curves for the best two GPR84 agonists, **38** and **57**, as well as for the known agonists decanoic acid and diindolylmethane (**1**) are displayed in Figure 4. The diindolylmethanes were additionally tested at the parent CHO cell line that does not express GPR84. While **1**, **38** and **57** show a concentration-dependent inhibition of forskolin-induced cAMP accumulation in CHO cells transfected

with the human GPR84, no inhibition is observed in non-transfected cells. This proves that the effects observed for the diindolylmethane derivatives are due to GPR84 activation.

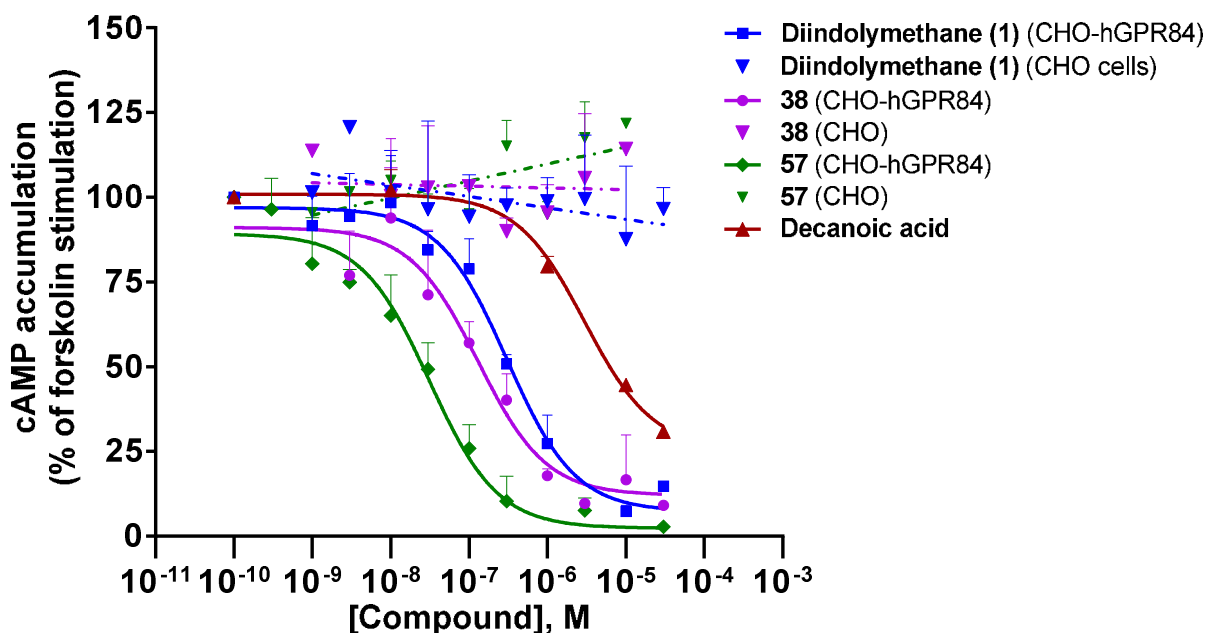


Figure 4. Concentration-response curves of selected GPR84 agonists determined in cAMP accumulation assays. Non-transfected CHO cells or CHO cells stably expressing the human GPR84 (CHO-hGPR84) were preincubated with the respective test compounds at the indicated concentrations for 5 min. Then 10 μ M forskolin was added and the cells were incubated for additional 15 min. The maximal forskolin-induced cAMP accumulation in the absence of agonist stimulation was defined as 100 %. EC₅₀ values for the investigated agonists were as follows: **38**: 80.0 nM, **57**: 41.3 nM; decanoic acid: 7420 nM, diindolylmethane: 252 nM. Mean values \pm SEM from 3 independent experiments performed in duplicates are shown.

In cAMP assays diindolylmethane (**1**) showed somewhat higher efficacy (125 %) than the standard agonist decanoic acid (set as 100 %, $p=0.0006$, ***). Most potent diindolylmethane derivatives and analogs displayed efficacies in the same range as **1**, e.g. for the most active compounds **38**, **52**, and **57** it ranged from 117-131 % of the maximal effect observed for decanoic acid. Only the 5,5'-dichloro-

1 diindolylmethane (**39**) showed a significantly lower efficacy of 86 % ($p=0.0002$, ^{***}) . These results
2
3 indicate that ligands binding to the diindolylmethane binding site induce effects on the receptor
4
5 conformation which lead to efficient G_i protein coupling.
6
7
8
9

10
11 Compounds which had not exhibited any agonistic activity in cAMP assays were tested for their ability
12
13 to block GPR84 activation. However, none of the compounds was found to act as an antagonist at
14
15 GPR84 at a concentration of 10 μ M (data not shown).
16
17
18
19

20 21 β -Arrestin assays

22
23
24 Selected GPR84 agonists identified in cAMP assays were further evaluated in β -arrestin assays (see
25
26 Table 8 and 9). We used the β -galactosidase complementation assay technology (DiscoverX[®]), since it
27
28 is highly specific for the expressed receptor. The human GPR84 containing a fragment of β -
29
30 galactosidase, and β -arrestin containing the complementary fragment of the functional enzyme are co-
31
32 expressed in CHO cells. When GPR84 is activated, β -arrestin is recruited resulting in the formation of a
33
34 functional enzyme.^{84,85} This assay hardly produces any artifacts. Moreover we could exclude potential
35
36 false-positive results by testing the compounds versus another GPCR, the fatty acid receptor FFAR4,
37
38 expressed in the same system.
39
40
41
42
43

44
45 As a control, we used the agonist embelin which is more suitable as a standard agonist in the β -arrestin
46
47 assay than decanoic acid since it is more potent in that assay and has a higher efficacy. Both lipidic
48
49 agonists displayed virtually identical potency in cAMP accumulation and β -arrestin translocation
50
51 assays, whereas **1** was 7-fold more potent in the G_i -dependent pathway as compared to β -arrestin
52
53 recruitment, even though the difference was not statistically significant ($p=0.1637$, ns). The SARs of
54
55 diindolylmethane derivatives determined in the β -arrestin assay were quite different from those
56
57 observed in the cAMP assays. Surprisingly, the two most potent compounds in cAMP assays, **38** and
58
59
60

57, activated GPR84 in the β -arrestin assay with only moderate potency, displaying 54-fold (**38**) and 132-fold (**57**, $p < 0.0001$, ****) lower potency than in the cAMP assay. In contrast, the agonists **34**, **37** and **95** that displayed only moderate potency in the cAMP assay were significantly more potent in the β -arrestin assay showing similar potency as the lead compound **1**. Moreover, some diindolylmethane derivatives that were found to be inactive in the cAMP assay exhibited significant agonistic activities in the β -arrestin assay, *i.e.*, compounds **50**, **60**, **77**, **78** and **80**. In particular, diindolylmethane derivatives with ethyl (**77**), propyl (**78**) or isopropyl (**80**) substitution at the 3,3'-methylene position (C10) activated GPR84-induced β -arrestin translocation with EC_{50} values in the low micromolar range, while the corresponding methyl (**75**) and butyl (**79**) derivatives did not show any effect at a concentration of 10 μ M. Thus, an ethyl substituent appears to possess the optimal size.

Concentration-response curves for the best GPR84 agonists in β -arrestin recruitment assays are shown in Figure 5.

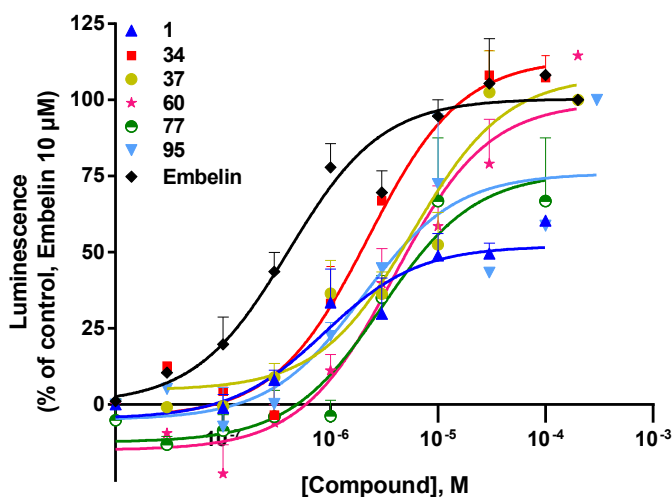


Figure 5. Concentration-response curves of GPR84 agonists determined in β -arrestin assays using the β -galactosidase complementation technology. The maximal luminescence induced by the standard agonist embelin (10 μ M) was defined as 100 %. EC_{50} values were calculated as follows: **1**: 1.64 μ M, **34**:

1.23 μ M, **37**: 1.20 μ M, **60**: 2.27, **77**: 2.97 μ M, **95**: 1.08 μ M, embelin: 0.400 μ M. Mean values \pm SEM from 3-4 independent experiments performed in duplicates are shown.

Diindolylmethane (**1**) displayed lower efficacy (60 %) in activating β -arrestin recruitment as compared to the standard agonists decanoic acid (92 %, $p=0.0477$, *) and embelin (set at 100 % $p=0.0028$, **). For the various diindolylmethane derivatives and analogs that activated the β -arrestin pathway large differences in efficacies could be observed ranging from 60 % (for **1**) to 385 % (for 5-F,7-F,5'-F,7'-F-diindolylmethane, **57**). The efficacy of the compounds was not correlated to their potency. The most efficacious compounds, besides **57**, were 5-F,6-Cl,5'-F,6'-Cl -diindolylmethane (**54**, 181 %) and 10-propyl-diindolylmethane (**78**, 199 %), whereas 6-F,6'-F-diindolylmethane (**49**, 48 %) displayed the lowest efficacy among the active compounds.

Biased agonism at GPCRs leads to the selective activation of specific downstream pathways and may therefore result in reduced side-effects. The development of biased ligands for GPR84 will allow future studies towards elucidating the consequences of selectively activating the one or the other pathway.

Allosteric mechanism of GPR84 activation by diindolylmethane derivatives

Although both, the lipid derivative decanoic acid and the heterocyclic small molecule diindolylmethane, behave as efficacious GPR84 agonists, it appears likely that they interact with different binding site on the receptor.⁴¹ The binding site of decanoic acid is considered to be the orthosteric binding site while diindolylmethane derivatives are supposed to be allosteric GPR84 agonists. To corroborate this assumption we performed cAMP accumulation experiments in GPR84-expressing CHO cells with various combinations of agonists as previously described for other GPCRs.⁸⁶

Concentration-response curves for decanoic acid were performed in the presence of different concentrations of decanoic acid (Figure 6A). As to be expected, the addition of the orthosteric agonist did not lead to a shift of the curve for decanoic acid. As shown in Figure 6B, the addition of diindolylmethane to decanoic acid resulted in an increase in efficacy (higher maximal inhibition of cAMP accumulation) as well as a significant leftward shift of the concentration-response curve for decanoic acid (EC_{50} values for **1** and **57** are depicted in Table 9). The effects increased with increasing concentration of **1**. These results indeed suggest that diindolylmethane binds to an allosteric binding site acting as an ago-allosteric modulator.⁸⁷ In the same setting, the more potent diindolylmethane derivative **57** displayed the same effects but with even higher potency and efficacy (Figure 6C and Table 9). The allosteric K_B values for decanoic acid in the presence of **1** and **57** were determined to be 880 nM and 634 nM, respectively. The cooperativity factor α on decanoic acid was calculated to be 1 for both compounds. As expected, diindolylmethane derivative **77** which was shown to act as a β -arrestin-biased agonist without effects on the G_i protein-dependent pathway did not display any effects on the concentration-response curve of decanoic acid (Figure 6D).

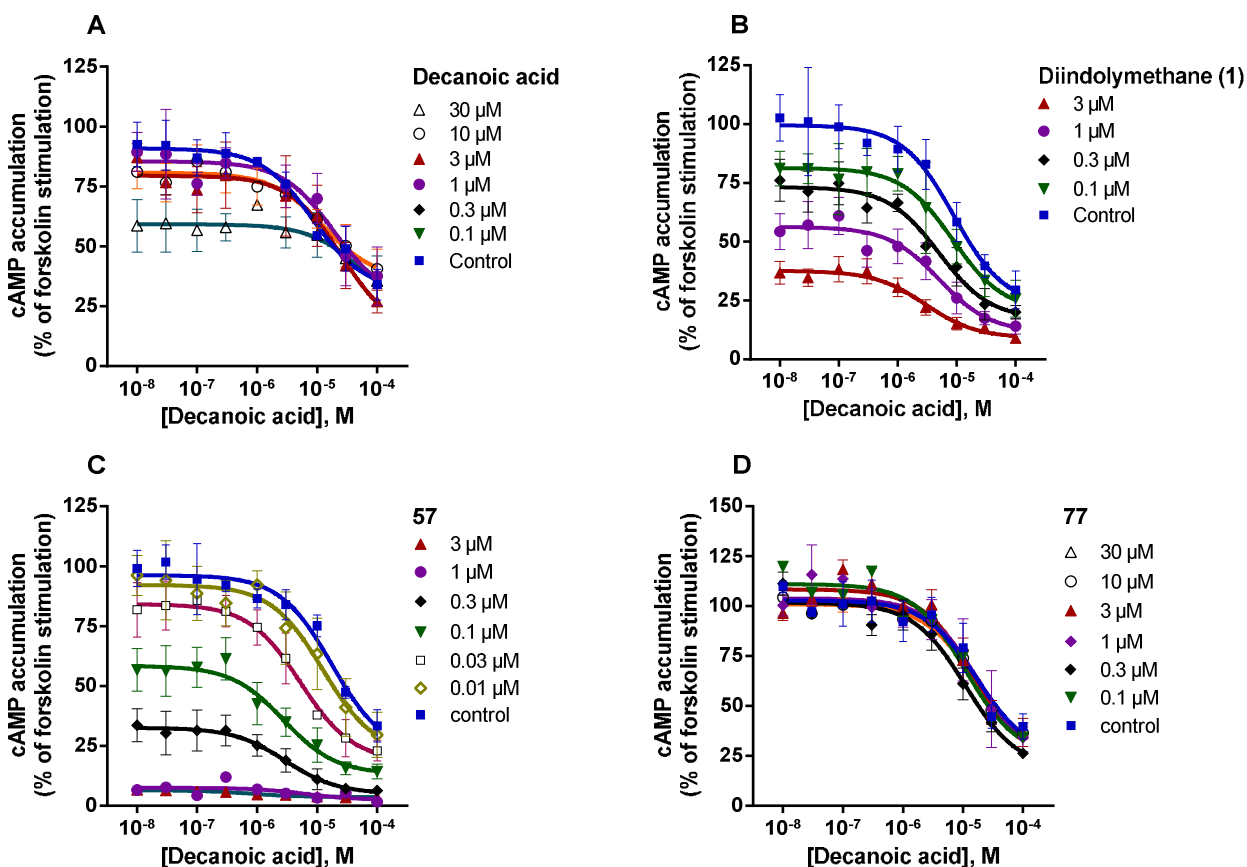


Figure 6. Allosteric interaction of diindolylmethane derivatives **1** and **57** with respect to the orthosteric agonist decanoic acid investigated in cAMP accumulation assays. Inhibition of forskolin-induced cAMP accumulation in GPR84-expressing CHO cells was measured in the presence of different concentrations of orthosteric and/or allosteric GPR84 agonists: (A) decanoic acid versus decanoic acid, (B) decanoic acid versus diindolylmethane, (C) decanoic acid versus diindolylmethane derivative **57**, and (D) decanoic acid versus diindolylmethane derivative **77**. Maximal forskolin-induced cAMP accumulation in the absence of test compound was defined as 100 %. Mean values \pm SEM from 3 independent experiments performed in duplicates are shown.

Table 9. Potency of decanoic acid in the absence and presence of diindolylmethane derivatives **1** or **57** at the human GPR84 determined in cAMP accumulation assays

Agonists	EC ₅₀ ± SEM of decanoic acid (n=3)
Decanoic acid alone	9.22 ± 1.03 μM
Decanoic acid + 0.1 μM 1	8.37 ± 0.97 μM
Decanoic acid + 0.3 μM 1	6.28 ± 1.06 μM
Decanoic acid + 1 μM 1	5.12 ± 0.95 μM*
Decanoic acid + 3 μM 1	2.88 ± 0.21 μM**
Decanoic acid alone	13.1 ± 0.62 μM
Decanoic acid + 0.01 μM 57	11.4 ± 2.49 μM
Decanoic acid + 0.03 μM 57	6.52 ± 0.77 μM**
Decanoic acid + 0.1 μM 57	2.68 ± 0.42 μM***
Decanoic acid + 0.3 μM 57	3.58 ± 1.35 μM*

*p < 0.05; ** p < 0.01; *** p< 0.005 (compared to decanoic acid in the absence of diindolylmethane derivative)

Receptor selectivity

In order to further investigate the selectivity of new GPR84 agonists, all compounds were tested at the human free fatty acid receptors FFAR1 (in calcium mobilization assays) and FFAR4 (in β-arrestin assays), which show overlapping preferences for medium chain fatty acids (see Table S2 and S3 in Supporting Information for results of the entire set of compounds). In agonist assays all tested compounds were virtually inactive at FFAR1 and FFAR4. In antagonist assays, some compounds showed weak antagonistic effects at FFAR1. Specifically, 4,4'-difluoro-diindolylmethane (**34**: EC₅₀ 6.49 μM), 10-propyl-diindolylmethane (**78**: EC₅₀ 8.81 μM) and 10-isobutyl-diindolylmethane (**80**: EC₅₀ 8.89 μM) displayed moderate FFAR1 inhibition (see Table S2). None of the tested compounds inhibited FFAR4 activity. Therefore, the identified and optimized potent GPR84 agonists can be considered to be selective for GPR84 versus FFAR1 and FFAR4. Selected diindolylmethane derivatives including **1**, **38**,

1 **57** and **77** were additionally investigated for their agonistic activity at the human GPR35, which is
2
3 phylogenetically related to GPR84. All tested GPR84 agonists were shown to be inactive at GPR35 at a
4
5 concentration of 10 μ M (see Table S4 in Supporting Information).
6
7
8
9

10 A well-known activity of **1** is its activation of the arylhydrocarbon receptor (AhR), a transcription factor
11 involved in gene regulation.⁴³ To study the selectivity of **1** and its optimized derivatives **38** and **57** for
12
13 GPR84 versus the AhR, we measured their effects on the expression of the AhR target gene Cyp1A1.
14
15 To this end, the well established human hepatocellular carcinoma cell line HepG2 was employed. The
16
17 cells were incubated with 5 μ M or 20 μ M of **1**, **38**, or **57**, or were left untreated. 3-Methylcholanthrene
18
19 (10 μ M) was used as positive control.⁸⁸ While **1** induced a robust concentration-dependent Cyp1A1
20
21 expression in HepG2 cells at 5 and 20 μ M, which was, however lower than that of 3-
22
23 methylcholanthrene, the optimized GPR84 agonist **38** showed only a weak response at a high
24
25 concentration of 20 μ M. The most potent GPR84 agonist of the present series, compound **57** did not
26
27 induce any significant AhR-activation (see Figure 7). Thus, in comparison to the lead structure **1**, the
28
29 developed diindolylmethane derivatives **38** and **57** are not only more potent at GPR84 but also
30
31 significantly more selective versus the AhR.
32
33
34
35
36
37
38
39
40
41
42
43
44
45
46
47
48
49
50
51
52
53
54
55
56
57
58
59
60

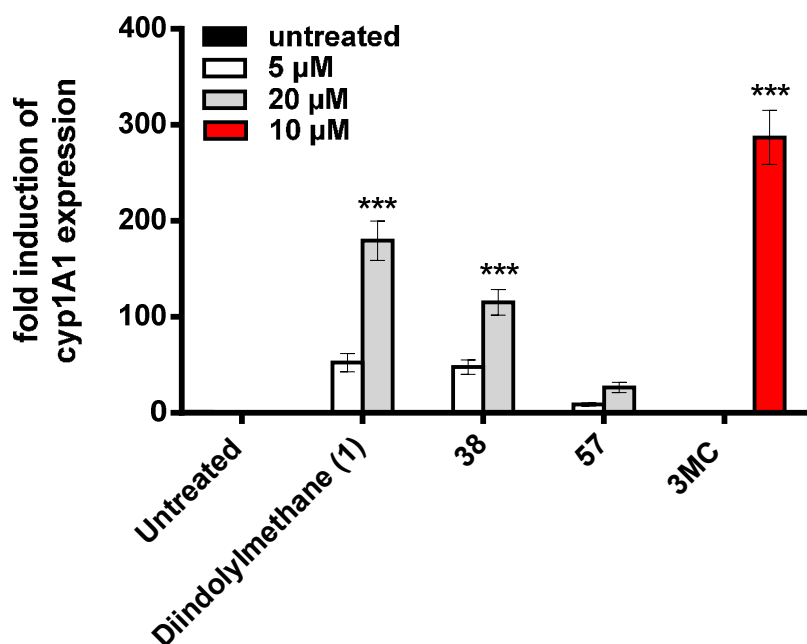


Figure 7. Arylhydrocarbon receptor activation-mediated induction of cytochrom P450 1A1 (cyp1A1) expression. HepG2 cells were stimulated with diindolymethane derivatives **1**, **38**, or **57** or 3-methylcholanthrene (3MC) as a positive control, respectively, for 18 h or were left untreated (negative control). Cyp1A1 levels were determined by quantitative real-time PCR ($p < 0.001$ One-way ANOVA with Sidak correction). Mean values \pm SEM from 3 independent experiments are shown.

Finally, we wanted to know whether the potent AhR activators 3-methylcholanthrene, indole-3-carbinol (3IC), a precursor of **1**, and 5,11-dihydroindolo[3,2-*b*]carbazole, a condensation product of **1**, are able to activate the human GPR84. In cAMP accumulation assays using CHO-hGPR84 cells none of the AhR ligands was able to inhibit forskolin-induced cAMP accumulation up to concentrations of 100 μ M (see Figure S1).

Chemical stability

Two of the most potent compounds, **38** and **52**, obtained in this study along with lead compound **1** were selected for studying their chemical stability at different pH values, (i) in simulated gastric fluid, (ii) in 1

mM sodium hydroxide solution (pH 11), (iii) in water and (iv) in 0.01% ammonia solution (pH 9). The experiments were conducted as previously reported.⁸⁹ The samples were incubated at 37 °C and analyzed by LC-MS after different time intervals of up to 24 h.

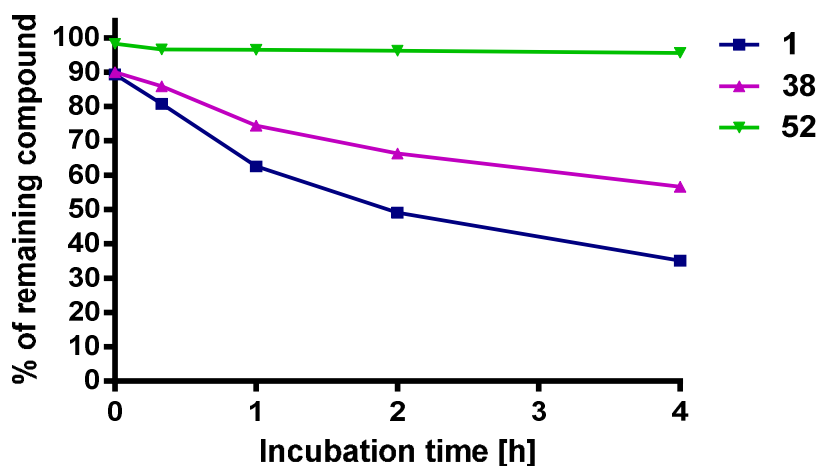


Figure 8. Stability of selected diindolylmethane derivatives in artificial gastric acid at 37 °C.

The analyses showed that all three compounds showed high stability in water as well as under basic conditions (see SI Figures S2-S4). However, the lead structure (**1**) was relatively unstable in artificial gastric acid consisting of hydrochloric acid, sodium chloride and pepsin (pH 1.2). After 1, 2 and 4 h of incubation 63, 49, and 35% of **1** were still intact. The 5,5'-difluoro-substituted diindolylmethane derivative **38** was more stable (57% remained intact after 4 h), while the 7,7'-difluoro-substituted derivative **52** was completely stable (see Figure 8 and SI Figure S1).

CONCLUSIONS

In conclusion, we have developed a simple and highly efficient method for the synthesis of a large variety of diindolylmethane derivatives and analogs. A series of 60 diindolylmethane and -methanone and 2-oxoindole derivatives were obtained, 28 of which (**34**, **35**, **43-46**, **51-57**, **76**, **77**, **83**, **85**, **86**, **93-97**, **105**, **108**, **111-113**) have not been previously reported, and 27 of which (**1**, **32**, **33**, **36-40**, **41**, **42**, **47-50**, **58-60**, **75**, **78-81**, **82**, **84**, **87**, **88** and **91**) have been reported in the literature, but were now synthesized

by an optimized procedure. Compounds **104**, **106**, **107**, **109** and **110** were obtained according to a reported method. SARs of the compounds as agonists of the potential therapeutic target GPR84 were analyzed and they were optimized for their potency to inhibit cAMP accumulation of the G_i -coupled receptor. 3,3'-Diindolylmethane derivatives bearing small substituents at the 5- or 7-position of the indole ring systems showed high GPR84 agonistic activity, while most larger substituents were not well tolerated. 5,5'-Difluoro- (**38**, EC_{50} 80.0 nM), 7,7'-difluoro- (**52**, EC_{50} 113 nM) and tetrafluoro-diindolylmethane (**57**, EC_{50} 41.3 nM) were found to be the most potent GPR84 agonists of the present series and they showed high efficacy. Measurements of effects of different concentrations of diindolylmethane and its derivative **57** on dose-response curves of the orthosteric agonist decanoic acid in cAMP assays indicated an ago-allosteric mechanism of action. Potencies of selected compounds were further determined in β -arrestin translocation assays indicating that **38**, **52** and **57** are biased towards G_i -mediated adenylate cyclase inhibition, in contrast to the lead structure **1** which addresses both pathways with equal potency. In contrast, compounds **50**, **60**, **77**, **78** and **80** were found to preferably activate β -arrestin recruitment. A range of different efficacies was observed in the β -arrestin assays for the differently substituted diindolylmethane derivatives. The consequences of biased behaviour of the new GPR84 agonists will have to be explored in further experiments, which are beyond the scope of the present study. The compounds displayed high selectivity for GPR84 versus the related fatty acid receptors FFAR1 and FFAR4, which show an overlapping ligand preference, as well as versus the phylogenetically related receptor GPR35. Importantly, in contrast to the lead structure **1**, the potent GPR84 agonist **57** did not show any activation of the arylhydrocarbon receptor. The new compounds will be useful tools for further elucidating the (patho)physiological roles of GPR84 and will allow for target validation studies.

EXPERIMENTAL SECTION

General Methods. All commercially available reagents were used as purchased (Acros, Alfa Aesar, Sigma-Aldrich, abcr or TCI). Solvents were used without additional purification or drying except for dichloromethane, which was distilled over calcium hydride. The reactions were monitored by thin layer chromatography (TLC) using aluminum sheets with silica gel 60 F₂₅₄ (Merck). Column chromatography was performed with silica gel 0.060-0.200 mm, pore diameter ca. 6 nm. For microwave reactions a CEM Focused Microwave Synthesis type Discover apparatus was used. All synthesized compounds were finally dried in vacuum at 8–12 Pa (0.08–0.12 mbar) using a sliding vane rotary vacuum pump (Vacuubrand GmbH). ¹H-, ¹³C NMR and ¹³C_{apt} NMR data were collected on a Bruker Avance 500 MHz NMR spectrometer at 500 MHz (¹H), or 126 MHz (¹³C), respectively. If indicated, NMR data were collected on a Bruker Ascend 600 MHz NMR spectrometer at 600 MHz (¹H), or 151 MHz (¹³C), respectively. DMSO-*d*₆ was employed as a solvent at 303 K, unless otherwise noted. Chemical shifts are reported in parts per million (ppm) relative to the deuterated solvent; that is, DMSO, δ ¹H: 2.49 ppm; ¹³C: 39.7 ppm. Coupling constants *J* are given in Hertz and spin multiplicities are given as s (singlet), d (doublet), t (triplet), q (quartet), sext. (sextet), m (multiplet), br (broad). Melting points were determined on a Büchi 530 melting point apparatus and are uncorrected. The purities of isolated products were determined by ESI-mass spectra obtained on an LCMS instrument (Applied Biosystems API 2000 LCMS/MS, HPLC Agilent 1100) using the following procedure: the compounds were dissolved at a concentration of 1.0 mg/mL in acetonitrile containing 2 mM ammonium acetate. Then, 10 μL of the sample were injected into an HPLC column (Macherey-Nagel Nucleodur® 3 μ C18, 50 x 2.00 mm). Elution was performed with a gradient of water/acetonitrile (containing 2 mM ammonium acetate) from 90:10 to 0:100 for 20 min at a flow rate of 300 μL/min, starting the gradient after 10 min. UV absorption was detected from 200 to 950 nm using a diode array detector. Purity of all compounds was determined by LC-UV-ESI-MS at 254 nm, and the purities of all tested compounds were found to be ≥ 95 %

Compounds **1**,⁶⁷ **32**,⁶⁷ **33**,⁶⁸ **36-40**,⁶⁷ **41**,⁶⁹ **42**,⁶⁷ **47-50**,⁶⁷ **58**,⁷⁰ **59**,⁶⁷ **60**,⁶⁷ **75**,⁷² **78-80**,⁷⁵⁻⁷⁶ **82**,⁵² **84**,⁵² **87**,⁷⁷ and **88**⁵² have previously been described but were now obtained by new methods. Compounds **91**,⁷⁸ **104**,⁸¹ **106**⁸² and **110**⁸² were synthesized as described in the literature. The synthesis and structural characterization data of the new compounds and their intermediates are described below.

General procedure for the preparation of 3,3'-diindolylmethanes (**32-60**)

A mixture of the appropriate indole (5 mmol) and formaldehyde (38 %) (2.5 mmol) in water (5 mL) was irradiated under microwave irradiation at 100 °C for the appropriate time. After completion of the reaction, the mixture was diluted with water (30 mL) and extracted with ethyl acetate (3 x 20 mL). The combined organic layers were washed with brine, dried over MgSO₄, filtered and evaporated under reduced pressure. The resulting crude product was purified by column chromatography on silica gel using a mixture of petroleum ether and ethyl acetate to obtain the pure product.

General procedure for the synthesis of **75-88**

Indole **2** (10 mmol) and the corresponding aldehyde (**61-74**) (5 mmol) were taken up in water (10 mL). Sodium dodecylsulfate (SDS, 10 % (w/w)) was added to the reaction mixture and then the mixture was allowed to stir until completion of the reaction at 100 °C under microwave irradiation. The mixture was washed with ethyl acetate (2 x 30 mL), dried over MgSO₄ and evaporated under reduced pressure. The product was purified by a column chromatography using petroleum ether and ethyl acetate as eluents.

Procedure for the synthesis of **91**

To a solution of indole (**2**, 10 mmol) in anhydrous dichloroethane (3 mL) at 0 °C under argon was added indole-3-carboxylic acid chloride (**90**), which was previously synthesized from the corresponding acid (**89**, 11 mmol) treated with thionyl chloride (0.5 mL), in dichloroethane (2 mL), by stirring under Argon. Followed by zirconium tetrachloride (13 mmol) was added under argon condition. The reaction temperature was then gradually increased to room temperature and continued the stirring for 4 h. After

1 completion of the reaction, resulting mixture was quenched with water (10 mL) and extracted with ethyl
2 acetate (2 x 20 mL). The combined organic layer was washed with brine, dried over magnesium sulfate,
3
4 filtered and evaporated under reduced pressure. Column chromatography purification on silica gel
5
6 eluting with EtOAc and petroleum ether provided the desired product.
7
8
9

10 11 12 **General procedure for the synthesis of 93–96**

13
14 After a mixture of TFAC (1 mmol) and DMSO (10 mmol) in dioxane (5 mL) was stirred at 0 °C under
15 an Argon atmosphere for 30 min, indole (**2**, 1 mmol) was added to the mixture and the mixture was
16
17 heated at 80 °C for 30 min. After cooling, corresponding indole derivative (**8**, **9**, **14** or **29**, 1 mmol) was
18
19 added to the mixture, which was then heated at 80 °C for 30 min. Cu(OAc)₂•H₂O (1 mmol) was added
20
21 next at 80 °C and the mixture was heated for 2 h. After cooling, the mixture was diluted with ethyl
22
23 acetate (100 mL), washed with 10 % aq. NaHCO₃ solution and brine, and dried over MgSO₄. The
24
25 solvent was removed, and the residue was separated by silica gel column chromatography
26
27
28
29
30
31
32

33 **General procedure for the synthesis of 104–109**

34
35 2-Oxindole (**98** or **99**, 37 mmol) was treated with the appropriate indolecarboxaldehyde (**100–103**, 41
36
37 mmol) and piperidine (16 mmol) in absolute ethanol. After the mixture was heated to 65 °C for 2 h, the
38
39 solvent was removed under reduced pressure. The residue was dissolved in water (50 mL) and extracted
40
41 with ethyl acetate (3 x 20 mL). The combined organic layer was washed with brine, dried over MgSO₄
42
43 and evaporated to dryness. The product was purified by silica gel column chromatography.
44
45
46
47
48
49

50 **General procedure for the synthesis of 110–113**

51
52 To a solution of the appropriate 2-oxindole derivative (**104–109**, 10 mmol) in ethanol (20 mL) was
53
54 added NaBH₄ (12 mmol) portionwise for 5-10 min at room temperature and the reaction mixture was
55
56 heated to 65 °C for 2 h. After completion of the reaction, the mixture was cooled down to rt and the
57
58 ethanol was removed under reduced pressure. The residue was dissolved in ice-water and extracted with
59
60

ethyl acetate (2 x 50 mL). The combined organic layers were washed with brine, dried over MgSO₄, filtered and evaporated under reduced pressure. The resulting product was purified by column chromatography using a mixture of petroleum ether and ethyl acetate.

Di-(4-fluoro-1*H*-indole-3-yl)methane (34). The compound was synthesized using 4-fluoroindole (**5**) and was isolated as a brown solid (82 % yield). ¹H NMR (500 MHz, DMSO-*d*₆) δ 10.99 (br s, 2H, NH), 7.15 (d, *J* = 8.1 Hz, 2H), 6.99 (t, *J* = 8.0, 5.1 Hz, 2H), 6.95 (d, *J* = 2.3 Hz, 2H), 6.71 – 6.63 (m, 2H), 4.28 (s, 2H). ¹³C NMR (126 MHz, DMSO-*d*₆) δ 157.71, 155.77, 139.40, 123.34, 121.46, 121.40, 115.41, 113.29, 108.09, 108.07, 103.42, 103.27, 23.09. LC-MS (m/z): positive mode 283 [M+H]¹⁺. Purity by HPLC UV (254 nm)-ESI-MS: 96 %. Mp: 142–144 °C.

Di-(4-chloro-1*H*-indole-3-yl)methane (35). The compound was synthesized using 4-chloroindole (**6**) and was isolated as a brown solid (86 % yield). ¹H NMR (600 MHz, DMSO-*d*₆) δ 11.06 (br s, 2H, NH), 7.32 (dd, *J* = 8.0, 0.9 Hz, 2H), 7.02 (t, *J* = 7.8 Hz, 2H), 6.95 (dd, *J* = 7.6, 0.9 Hz, 2H), 6.86 (dd, *J* = 2.4, 1.2 Hz), 4.61 (s, 2H). ¹³C NMR (151 MHz, DMSO-*d*₆) δ 138.23, 125.26, 125.04, 123.52, 121.70, 119.17, 115.12, 110.87, 23.56. LC-MS (m/z): positive mode 313 [M-2H]²⁺. Purity by HPLC UV (254 nm)-ESI-MS: 95 %. Mp: 172–174 °C.

Di-(5-methylcarboxylate-1*H*-indole-3-yl)methane (43). The compound was synthesized using methyl indole-5-carboxylate (**14**) and was isolated as a brown solid (84 % yield). ¹H NMR (600 MHz, DMSO-*d*₆) δ 11.18 (br s, 2H, NH), 8.23 – 8.19 (m, 2H), 7.69 (dd, *J* = 8.6, 1.6 Hz, 2H), 7.41 (dd, *J* = 8.4, 0.7 Hz, 2H), 7.22 (d, *J* = 2.2 Hz), 4.22 (d, *J* = 1.1 Hz, 2H), 3.79 (s, 6H). ¹³C NMR (151 MHz, DMSO-*d*₆) δ 167.41, 139.19, 126.80, 124.86, 122.07, 121.41, 119.84, 115.56, 111.49, 51.69, 20.68. LC-MS (m/z): positive mode 363 [M+H]¹⁺. Purity by HPLC UV (254 nm)-ESI-MS: >98 %. Mp: 231–233 °C.

Di-(5-formyl-1*H*-indole-3-yl)methane (44). The compound was synthesized using indole-5-carboxaldehyde (**15**) and was isolated as a brown solid (85 % yield). ¹H NMR (500 MHz, DMSO-*d*₆) δ 11.34 – 11.30 (br s, 2H, NH), 9.93 (s, 2H), 8.18 (d, *J* = 1.4 Hz, 2H), 7.60 (dd, *J* = 8.5, 1.5 Hz, 2H), 7.48 (d, *J* = 8.5 Hz, 2H), 7.33 (d, *J* = 2.2 Hz, 2H), 4.28 (s, 2H). ¹³C NMR (126 MHz, DMSO-*d*₆) δ 192.51, 140.00, 128.40, 127.06, 125.25, 124.23, 121.12, 116.18, 112.22, 20.68. LC-MS (m/z): positive mode 203 [M+H]⁺. Purity by HPLC UV (254 nm)-ESI-MS: 99 %. Mp: 210–212 °C.

Di-(5-carboxyl-1*H*-indole-3-yl)methane (45). The compound was synthesized using indole-5-carboxylic acid (**16**) and was isolated as a brown solid (79 % yield). ¹H NMR (600 MHz, DMSO-*d*₆) δ 12.27 (br s, 2H, COOH), 11.12 (br s 2H, NH), 8.17 (d, *J* = 1.8 Hz, 2H), 7.67 (dd, *J* = 8.6, 1.7 Hz, 2H), 7.37 (d, *J* = 8.5 Hz, 2H), 7.22 (d, *J* = 2.2 Hz, 2H), 4.21 (s, 2H). ¹³C NMR (151 MHz, DMSO-*d*₆) δ 168.57, 139.10, 126.81, 124.62, 122.37, 121.58, 120.90, 115.44, 111.24, 39.28. LC-MS (m/z): positive mode 335 [M+H]⁺. Purity by HPLC UV (254 nm)-ESI-MS: >98 %. Mp: >300 °C.

Di-(5-benzyloxy-1*H*-indole-3-yl)methane (46). The compound was synthesized using 5-benzyloxyindole (**17**) and was isolated as a brown solid (75 % yield). ¹H-NMR (600 MHz; DMSO-*d*₆) δ 10.53 (br s, 2H, NH), 7.39-7.44 (m, 4H), 7.33-7.38 (m, 4H), 7.26-7.32 (m, 2H), 7.20 (d, *J* = 8.0 Hz, 2H), 7.12 (d, *J* = 2.4 Hz, 1H, 2-H), 7.07 (d, *J* = 2.4 Hz, 2H), 6.76 (d, *J* = 2.5 Hz, 1H), 6.75 (d, *J* = 2.5 Hz, 1H), 5.02 (s, 4H), 4.02 (s, 2H). ¹³C-NMR (151 MHz, DMSO-*d*₆) δ 151.8, 137.9, 131.8, 128.4, 127.8, 127.7, 127.6, 123.6, 114.1, 111.9, 111.5, 102.3, 70.3, 20.9. LC-MS (m/z): positive mode 459 [M+H]⁺. Purity by HPLC UV (254 nm)-ESI-MS: >98 %. Mp: 125–127 °C.

Di-(7-methoxy-1*H*-indole-3-yl)methane (51). The compound was synthesized using 7-methoxyindole (**22**) and was isolated as a brown solid (93 % yield). ¹H NMR (500 MHz, DMSO-*d*₆) δ 10.87 – 10.63 (m, 2H), 7.10 (d, *J* = 7.9 Hz, 2H), 6.99 (d, *J* = 2.4 Hz, 2H), 6.84 (t, *J* = 7.8 Hz, 2H), 6.59 (d, *J* = 7.6 Hz, 2H), 4.07 (s, 2H), 3.87 (s, 6H). ¹³C NMR (126 MHz, DMSO-*d*₆) δ 14.20, 20.86, 55.13, 100.55, 101.34,

101.49, 111.75, 111.84, 118.68, 122.49, 122.82, 126.50, 128.83, 146.19. LC-MS (m/z): positive mode
307 [M+H]¹⁺. Purity by HPLC UV (254 nm)-ESI-MS: >98 %. Mp: 166-168 °C.

Di-(7-fluoro-1*H*-indole-3-yl)methane (52). The compound was synthesized using 7-fluoroindole (**23**) and was isolated as a brown solid (85 % yield). ¹H NMR (500 MHz, DMSO-*d*₆) δ 11.21 (br s, 2H, NH), 7.32 (d, *J* = 1.4 Hz, 2H), 7.20 (d, *J* = 2.3 Hz, 2H), 6.90 – 6.88 (m, 2H), 6.88 – 6.85 (m, 2H), 4.12 (s, 2H). ¹³C NMR (126 MHz, DMSO-*d*₆) δ 150.30, 148.37, 131.27, 124.15, 118.49, 114.99, 105.80, 20.92. LC-MS (m/z): positive mode 283 [M+H]¹⁺. Purity by HPLC UV (254 nm)-ESI-MS: 96 %. Mp: 159-161 °C.

Di-(4,5-dichloro-1*H*-indole-3-yl)methane (53). The compound was synthesized using 4,6-dichloroindole (**24**) and was isolated as a brown solid (83 % yield). ¹H-NMR (500 MHz, DMSO-*d*₆) δ 11.21 (br s, 2H, NH), 7.39 (d, *J* = 2.9 Hz, 2H), 7.03 (d, *J* = 2.4 Hz, 2H), 6.92 (dd, *J* = 2.4, 1.1 Hz, 2H), 4.54 (s, 2H). ¹³C NMR (126 MHz, DMSO-*d*₆) δ 138.01, 126.41, 125.62, 125.41, 122.47, 119.02, 115.16, 115.63, 110.63, 23.12. LC-MS (m/z): positive mode 385 [M+H]⁺. Purity by HPLC UV (254 nm)-ESI-MS: >95 %. Mp: 171–173 °C.

Di-(5-fluoro-6-chloro-1*H*-indole-3-yl)methane (54). The compound was synthesized using 5-fluoro-6-chloroindole (**25**) and was isolated as a brown solid (76 % yield). ¹H NMR (500 MHz, DMSO-*d*₆) δ 10.95 (br s, 2H, NH), 7.46 (d, *J* = 6.4 Hz, 2H), 7.43 (d, *J* = 10.3 Hz, 2H), 7.33 (d, *J* = 2.4 Hz, 2H), 4.05 (s, 2H). ¹³C NMR (126 MHz, DMSO-*d*₆) δ 152.32, 150.46, 132.88, 126.16, 126.00, 114.50, 113.20, 112.94, 112.44, 104.96, 104.78, 20.54: LC-MS (m/z): positive mode 349 [M-2H]²⁻. Purity by HPLC UV (254 nm)-ESI-MS: >98 %. Mp: 225–227 °C.

Di-(4,5-difluoro-1*H*-indole-3-yl)methane (55). The compound was synthesized using 4,5-difluoroindole (**26**) and was isolated as a brown oil (87 % yield). ¹H NMR (600 MHz, DMSO-*d*₆) δ

11.16 (br s, 2H, NH), 7.43 (dd, $J = 11.5, 8.0$ Hz, 2H), 7.31–7.28 (m, 2H), 7.28–7.24 (m, 2H), 4.04 (s, 2H). ^{13}C NMR (151 MHz, DMSO- d_6) δ 145.80, 144.02, 131.44, 124.92, 124.95, 122.56, 114.38, 105.26, 24.22. LC-MS (m/z): negative mode 317 $[\text{M}-1\text{H}]^{1-}$. Purity by HPLC UV (254 nm)-ESI-MS: >95 %. Mp: 117–119 °C.

Di-(5,6-difluoro-1*H*-indole-3-yl)methane (56). The compound was synthesized using 5,6-difluoroindole (**27**) and was isolated as a brown solid (83 % yield). ^1H NMR (600 MHz, DMSO- d_6) δ 7.43 (dd, $J = 11.5, 8.0$ Hz, 2H), 7.32 – 7.28 (m, 2H), 7.28 – 7.24 (m, 2H), 4.04 (d, $J = 1.0$ Hz, 2H). ^{13}C NMR (151 MHz, DMSO- d_6) δ 147.38, 145.81, 131.45, 124.98, 124.96, 122.57, 105.26, 105.14, 99.34, 99.20, 21.15, 20.67. LC-MS (m/z): negative mode 317 $[\text{M}-1\text{H}]^1$. Purity by HPLC UV (254 nm)-ESI-MS: >98 %. Mp: 122–124 °C.

Di-(5,7-difluoro-1*H*-indole-3-yl)methane (57). The compound was synthesized using 5,7-difluoroindole (**28**) and was isolated as a brown solid (80 % yield). ^1H NMR (600 MHz, DMSO- d_6) δ 11.66 – 11.12 (m, 2H), 7.36 (d, $J = 2.5$ Hz, 2H), 7.14 (dd, $J = 9.5, 2.2$ Hz, 2H), 6.88 (dd, $J = 11.6, 9.6$ Hz, 2H), 4.06 (s, 2H). ^{13}C NMR (151 MHz, DMSO- d_6) δ 156.00, 154.70, 149.20, 147.47, 129.85, 126.16, 121.00, 115.41, 99.68, 95.91, 20.61. LC-MS (m/z): positive mode 331.3 $[\text{M}+\text{H}]^{1+}$. Purity by HPLC UV (254 nm)-ESI-MS: 96 %. Mp: 158–160 °C.

Di-(4-fluoro-1*H*-indole-3-yl)ethane (76). The compound was synthesized by reaction of 4-fluoroindole (**6**) with acetaldehyde (**61**) and was isolated as a brown solid (83 % yield). ^1H NMR (600 MHz, DMSO- d_6) δ 10.98 (s, 2H), 7.14 (d, $J = 8.1$ Hz, 2H), 6.98 (dd, $J = 7.9, 5.0$ Hz, 2H), 6.90 (d, $J = 2.3$ Hz, 2H), 6.63 (dd, $J = 11.5, 7.8$ Hz, 2H), 4.82 (q, $J = 7.1$ Hz, 1H), 1.66 (d, $J = 7.1$ Hz, 3H). ^{13}C NMR (151 MHz, DMSO- d_6) δ 157.33, 155.71, 139.52, 124.74, 122.26, 121.40, 119.56, 114.85, 108.04, 103.46, 29.19, 23.37. LC-MS (m/z): positive mode 295.5 $[\text{M}+\text{H}]^{1+}$. Purity by HPLC UV (254 nm)-ESI-MS: >95 %. Mp: 155–157 °C.

Di-(indole-3-yl)propane (77). The compound was synthesized by reaction of indole (**2**) with propionaldehyde and was isolated as a light blue solid (80 % yield); ^1H NMR (600 MHz, CDCl_3 -*d*) δ 7.89 (s, 2H), 7.57 (d, $J = 7.9$ Hz, 2H), 7.32 (d, $J = 8.2$ Hz, 2H), 7.24 (d, $J = 6.7$ Hz, 2H), 7.12 (t, $J = 7.7$ Hz, 2H), 7.03 – 6.97 (m, 2H), 4.36 (t, $J = 7.5$ Hz, 1H), 2.29 – 2.16 (m, 2H), 0.99 (td, $J = 7.4, 2.8$ Hz, 3H). ^{13}C NMR (151 MHz, CDCl_3 -*d*) δ 13.07, 28.66, 35.89, 76.79, 110.99, 118.96, 119.70, 120.35, 121.40, 121.70, 127.22, 136.58. LC-MS (*m/z*): negative mode 273 $[\text{M-H}]^-$. Purity by HPLC UV (254 nm)-ESI-MS: 96 %. Mp: 122–124 °C.

3,3'-Diindolyl-(*p*-hydroxyphenyl)methane (83). The compound was synthesized by reaction of indole (**2**, 10 mmol) with 4-hydroxybenzaldehyde (**69**, 5 mmol) and was isolated as a red solid (93 % yield). ^1H NMR (500 MHz, CDCl_3 -*d*) δ 7.91 (s, 1H, NH), 7.38 – 7.31 (m, 2H), 7.29 – 7.24 (m, 2H), 7.16 (dd, $J = 8.1, 7.1$ Hz, 2H), 7.00 (dd, $J = 8.0, 7.0$ Hz, 2H), 6.97 – 6.91 (m, 4H), 6.61 (dd, $J = 2.4, 1.0$ Hz, 2H), 5.86 (s, 1H). ^{13}C NMR (126 MHz, chloroform- d_3) δ 160.41, 139.68, 139.65, 136.68, 130.07, 130.01, 126.90, 123.54, 121.99, 119.82, 119.52, 119.27, 115.00, 114.84, 111.07, 39.44. LC-MS (*m/z*): positive mode 337 $[\text{M-2H}]^{2-}$ and negative mode 336 $[\text{M-1H}]^{1-}$. Purity by HPLC UV (254 nm)-ESI-MS: >97 %. Mp: 233–235 °C.

3,3'-Diindolyl-(*p*-fluorophenyl)methane (85). The compound was synthesized by reaction of indole (**2**, 10 mmol) with 4-fluorobenzaldehyde (**71**, 5 mmol) and was isolated as a red solid (80 % yield). ^1H NMR (600 MHz, $\text{DMSO-}d_6$) δ 10.73 (br s, 2H, NH), 7.32 (d, $J = 8.1$ Hz, 2H), 7.25 (d, $J = 7.9$ Hz, 2H), 7.17 – 7.06 (m, 2H), 7.01 (dd, $J = 8.2, 6.9$ Hz, 2H), 6.84 (dd, $J = 8.0, 6.9$ Hz, 2H), 6.80 – 6.73 (m, 2H), 6.70 – 6.54 (m, 2H), 5.70 (s, 1H). ^{13}C NMR (151 MHz, $\text{DMSO-}d_6$) δ 155.42, 136.75, 135.36, 129.28, 126.83, 123.53, 120.92, 119.33, 118.84, 118.21, 114.91, 111.53, 59.91. LC-MS (*m/z*): negative mode 339 $[\text{M-1H}]^{1-}$. Purity by HPLC UV (254 nm)-ESI-MS: >95 %. Mp: 78–80 °C.

3,3'-Diindolyl-(1,3-benzodioxol-4-yl)methane (86). The compound was synthesized by reaction of indole (**2**, 10 mmol) with 1,3-benzodioxole-4-carbaldehyde (**72**, 5 mmol) and was isolated as a yellow solid (91 % yield). ^1H NMR (600 MHz, $\text{DMSO-}d_6$) δ 10.78 (br s, 2H, NH), 7.33 (dd, $J = 8.2, 0.9$ Hz, 2H), 7.28 (dd, $J = 7.9, 1.1$ Hz, 2H), 7.02 (dd, $J = 8.0, 6.9$ Hz, 2H), 6.89 – 6.84 (m, 2H), 6.83 (m, 3H), 6.78 (d, $J = 7.9$ Hz, 1H), 5.93 (s, 2H), 5.75 (s, 1H). ^{13}C NMR (151 MHz, $\text{DMSO-}d_6$) δ 147.11, 145.31, 139.24, 136.73, 126.73, 123.62, 121.22, 121.00, 119.25, 118.32, 118.31, 111.58, 108.92, 107.90, 107.90, 100.78, 59.90. LC-MS (m/z): positive mode 337 $[\text{M-2H}]^{2-}$ and negative mode 336 $[\text{M-1H}]^{1-}$. Purity by HPLC UV (254 nm)-ESI-MS: 99 %. Mp: 106–108 °C.

3-(1*H*-Indol-3-ylmethyl)-1-methyl-1*H*-indole (93). The compound was synthesized by reaction of indole (**2**, 1 mmol) with 1-methylindole (**29**, 1 mmol) and was isolated as a yellow solid (40 % yield). ^1H NMR (500 MHz, $\text{DMSO-}d_6$) δ 10.71 (br s, 1H, NH), 7.52 (dd, $J = 18.0, 7.9$ Hz, 2H), 7.32 (dd, $J = 11.6, 8.2$ Hz, 2H), 7.13 (d, $J = 2.3$ Hz, 1H), 7.09 (dd, $J = 8.2, 6.8$ Hz, 1H), 7.06 (s, 1H), 7.05 – 6.97 (m, 1H), 6.93 (dd, $J = 20.4, 7.4$ Hz, 2H), 4.11 (s, 2H), 3.69 (s, 3H). ^{13}C NMR (126 MHz, $\text{DMSO-}d_6$) δ 136.89, 136.51, 127.60, 127.25, 122.90, 120.99, 120.86, 118.95, 118.69, 118.22, 118.16, 114.12, 113.76, 111.40, 32.29, 20.79. LC-MS (m/z): positive mode 261 $[\text{M+H}]^{1+}$. Purity by HPLC UV (254 nm)-ESI-MS: 97 %. Mp: 125–127 °C.

3-(1*H*-Indol-3-ylmethyl)-5-methoxy-1*H*-indole (94). The compound was synthesized by reaction of indole (**2**, 1 mmol) with 5-methoxyindole (**8**, 1 mmol) and was isolated as a brown solid (47 % yield). ^1H NMR (500 MHz, $\text{DMSO-}d_6$) δ 10.70 (br s, 1H, NH), 7.64 (d, $J = 7.5$ Hz, 1H), 7.34 (d, $J = 8.1$ Hz, 1H), 7.23 (d, $J = 9.2$ Hz, 1H), 7.20 (t, $J = 7.5$ Hz, 1H), 7.11 (t, $J = 7.5$ Hz, 1H), 7.07 (s, 1H), 6.89 (s, 2H), 6.86 (d, $J = 8.6$ Hz, 1H), 4.21 (s, 2H), 3.81 (s, 3H). ^{13}C NMR (151 MHz, $\text{DMSO-}d_6$) δ 153.91, 136.62, 131.70, 128.04, 127.73, 123.27, 122.39, 122.01, 119.34, 119.25, 115.72, 115.41, 112.24,

111.92, 111.21, 101.23, 56.03, 21.41. LC-MS (m/z): positive mode 297 [M+H]¹⁺. Purity by HPLC UV (254 nm)-ESI-MS: 95 %. Mp: 102–104 °C.

3-((1*H*-Indol-3-yl)methyl)-5-fluoro-1*H*-indole (95). The compound was synthesized by reaction of indole (**2**, 1 mmol) with 5-fluoroindole (**9**, 1 mmol) and was isolated as a brown solid (41 % yield). ¹H NMR (500 MHz, DMSO-*d*₆) δ 10.89 – 10.46 (m, 2H, NH), 7.50 (d, *J* = 7.8 Hz, 1H), 7.33 – 7.26 (m, 2H), 7.21 (dd, *J* = 5.2, 2.6 Hz, 2H), 7.16 (d, *J* = 2.3 Hz, 1H), 7.02 (dd, *J* = 8.1, 6.9 Hz, 1H), 6.91 (dd, *J* = 7.9, 6.9 Hz, 1H), 6.85 (dd, *J* = 9.2, 2.6 Hz, 1H), 4.09 (s, 2H). ¹³C_{apt} NMR (126 MHz, DMSO-*d*₆) δ 155.66, 136.53, 133.17, 127.26, 125.02, 122.92, 122.85, 120.87, 120.83, 118.74, 118.15, 118.12, 114.66, 114.00, 112.32, 112.25, 111.42, 20.94. LC-MS (m/z): positive mode 263 [M-H]¹⁻. Purity by HPLC UV (254 nm)-ESI-MS: 97 %. Mp: 141–143 °C.

Methyl 3-((1*H*-indol-3-yl)methyl)-1*H*-indole-5-carboxylate (96). The compound was synthesized by reaction of indole (**2**, 1 mmol) with methyl indole-5-carboxylate (**14**, 1 mmol) and was isolated as a brown solid (35 % yield). ¹H NMR (600 MHz, DMSO-*d*₆) δ 10.72 (br s, 2H, NH), 8.20 (d, *J* = 1.5 Hz, 1H), 7.68 (dd, *J* = 8.5, 1.7 Hz, 1H), 7.50 (dd, *J* = 8.0, 1.1 Hz, 1H), 7.39 (d, *J* = 8.5 Hz, 1H), 7.31 (dd, *J* = 8.3, 0.9 Hz, 1H), 7.26 (d, *J* = 2.2 Hz, 1H), 7.09 – 7.00 (m, 2H), 6.91 (dd, *J* = 8.0, 7.0 Hz, 1H), 4.18 (s, 2H), 3.79 (s, 3H, CH₃). ¹³C NMR (151 MHz, DMSO-*d*₆) δ 167.45, 139.19, 136.57, 127.23, 126.91, 124.88, 122.88, 122.00, 121.45, 120.98, 119.76, 118.74, 115.87, 113.96, 111.49, 111.44, 51.71, 20.90. LC-MS (m/z): positive mode 305 [M+H]¹⁺. Purity by HPLC UV (254 nm)-ESI-MS: 95 %. Mp: 146–148 °C.

3-((1*H*-indol-3-yl)methyl)-1*H*-indole-5-carboxylic acid (97). To a solution of compound **96** (10 mmol) in ethanol (10 mL) was added 2N NaOH (2 mL) and the resulting mixture was heated to reflux for 1 h. After completion of the reaction, ethanol was removed under reduced pressure, the pH was adjusted to 4–5, and the product was filtered, washed with H₂O and dried under vacuum. The compound

was isolated as a light brown solid (99 % yield). ^1H NMR (600 MHz, DMSO-d_6) δ 12.25 (s, 1H, COOH), 10.73 (br s, 1H, NH), 8.19 (s, 1H), 7.66 (dd, J = 8.4, 1.6 Hz, 1H), 7.50 (d, J = 7.9 Hz, 1H), 7.36 (d, J = 8.5 Hz, 1H), 7.31 (d, J = 8.1 Hz, 1H), 7.24 (d, J = 2.3 Hz, 1H), 7.09 (d, J = 2.3 Hz, 1H), 7.02 (t, J = 7.6 Hz, 1H), 6.91 (d, J = 7.5 Hz, 1H), 4.16 (s, 2H). ^{13}C NMR (151 MHz, DMSO-d_6) δ 168.48 (COOH), 139.05, 136.56, 127.24, 126.86, 124.59, 122.88, 121.58, 120.95, 118.75, 118.22, 115.76, 114.00, 111.48, 111.16, 20.96. LC-MS (m/z): positive mode 291 $[\text{M}+\text{H}]^{1+}$. Purity by HPLC UV (254 nm)-ESI-MS: 98 %. Mp: 244–246°C.

(*E/Z*)-3-((5-Fluoro-1*H*-indol-3-yl)methylene)indoline-2-one (105). The compound was synthesized by reaction of 2-oxindole (**98**, 37 mmol) with 5-fluoroindole-3-carbaldehyde (**101**, 41 mmol) and was isolated as a yellow solid (69 % yield). ^1H NMR (500 MHz, DMSO-d_6) δ 8.10 (s, 1H), 8.03 (dd, J = 10.1, 2.5 Hz, 1H), 7.90 (dd, J = 7.6, 1.1 Hz, 1H), 7.51 (dd, J = 8.8, 4.6 Hz, 1H), 7.13 (dd, J = 7.5, 1.1 Hz, 1H), 7.06 (dd, J = 9.1, 2.5 Hz, 1H), 6.98 (dd, J = 7.5, 1.0 Hz, 1H), 6.86 – 6.78 (m, 2H). ^{13}C NMR (126 MHz, DMSO-d_6) δ 168.20, 159.33, 139.35, 135.14, 132.60, 129.28, 127.11, 126.98, 125.78, 120.64, 119.51, 119.05, 113.54, 113.47, 111.66, 110.73, 110.52. LC-MS (m/z): positive mode 279 $[\text{M}+\text{H}]^{1+}$. Purity by HPLC UV (254 nm)-ESI-MS: 98 %. Mp: 279–281 °C.

(*E/Z*)-3-((5-Methoxy-1*H*-indol-3-yl)methylene)-5-fluoroindoline-2-one (108). The compound was synthesized by reaction of 5-fluoro-2-oxindole (**99**, 37 mmol) and 5-methoxyindole-3-carbaldehyde (**102**, 41 mmol) and was isolated as a yellow solid (80 % yield). ^1H NMR (500 MHz, DMSO-d_6) δ 10.45 (s, 1H), 8.19 (s, 1H), 7.86 (dd, J = 9.4, 2.6 Hz, 1H), 7.76 (d, J = 2.4 Hz, 1H), 7.40 (d, J = 8.7 Hz, 1H), 6.92 (dd, J = 9.7, 8.4 Hz, 1H), 6.86 (dd, J = 8.7, 2.4 Hz, 1H), 6.79 (dd, J = 8.4, 4.5 Hz, 1H), 3.88 (s, 3H). ^{13}C NMR (126 MHz, DMSO-d_6) δ 168.35, 159.03, 155.32, 135.27, 134.75, 131.07, 130.91, 129.92, 129.40, 129.38, 129.34, 127.65, 118.01, 114.25, 113.53, 113.14, 112.66, 112.61, 112.47, 111.56, 109.92, 109.55, 109.49, 109.25, 106.16, 105.95, 101.06, 55.80. LC-MS (m/z): positive mode 309 $[\text{M}+\text{H}]^{1+}$. Purity by HPLC UV (254 nm)-ESI-MS: 96 %. Mp: 296–298°C.

(*E/Z*)-3-((1*H*-Indol-5-yl)methylene)indoline-2-one (109). The compound was synthesized by reaction of 2-oxindole (**98**, 37 mmol) with indole-5-carbaldehyde (**103**, 41 mmol) and was isolated as a brown solid (73 % yield). ¹H NMR (500 MHz, DMSO-*d*₆) δ 11.37 (d, *J* = 19.4 Hz, 1H), 10.50 (s, 1H), 8.85 – 8.80 (m, 0H), 8.30 (dd, *J* = 8.7, 1.6 Hz, 0H), 7.96 (d, *J* = 1.5 Hz, 1H), 7.88 (s, 0H), 7.76 (d, *J* = 7.1 Hz, 2H), 7.69 (d, *J* = 7.6 Hz, 0H), 7.57 – 7.47 (m, 2H), 7.47 – 7.36 (m, 2H), 7.20 (td, *J* = 7.7, 1.1 Hz, 1H), 7.15 (td, *J* = 7.6, 1.1 Hz, 0H), 6.97 (td, *J* = 7.5, 0.9 Hz, 0H), 6.90 – 6.84 (m, 2H), 6.84 – 6.77 (m, 1H), 6.60 – 6.48 (m, 1H), 5.74 (s, 0H). ¹³C_{apt} NMR (126 MHz, DMSO-*d*₆) δ 169.26, 167.61, 155.60, 142.62, 140.09, 139.76, 138.80, 137.39, 136.86, 129.45, 127.86, 127.73, 126.99, 126.79, 126.34, 126.19, 125.96, 125.75, 125.20, 124.75, 123.04, 122.89, 122.82, 121.90, 121.70, 121.06, 120.89, 119.04, 111.86, 111.23, 110.04, 109.17, 102.62, 102.17, 46.78. LC-MS (m/z): positive mode 261 [M+H]¹⁺. Purity by HPLC UV (254 nm)-ESI-MS: >98 %. Mp: 153–155 °C.

3-((5-Methoxy-1*H*-indol-3-yl)methyl)indolin-2-one (110). The compound was synthesized from **106** (5 mmol) and was isolated as a light yellow solid (89 % yield). ¹H NMR (500 MHz, DMSO-*d*₆) δ 10.57 – 10.52 (m, 1H), 10.20 (s, 1H), 7.15 (d, *J* = 8.7 Hz, 1H), 7.06 (t, *J* = 7.6 Hz, 1H), 7.01 – 6.96 (m, 2H), 6.86 (d, *J* = 2.5 Hz, 1H), 6.81 (td, *J* = 7.5, 1.0 Hz, 1H), 6.69 (d, *J* = 7.7 Hz, 1H), 6.65 (dd, *J* = 8.7, 2.5 Hz, 1H), 3.76 (dd, *J* = 7.6, 4.7 Hz, 1H), 3.72 (s, 3H), 3.40 – 3.33 (m, 1H), 3.08 (dd, *J* = 14.7, 7.5 Hz, 1H). ¹³C_{apt} NMR (126 MHz, DMSO-*d*₆) δ 178.78, 152.99, 142.91, 131.18, 129.96, 127.66, 127.49, 124.43, 124.31, 120.94, 111.89, 111.11, 109.03, 100.59, 55.39, 46.00, 25.50. LC-MS (m/z): positive mode 291 [M+H]¹⁺. Purity by HPLC UV (254 nm)-ESI-MS: 96 %. Mp: 223–225 °C.

5-Fluoro-3-((5-fluoro-1*H*-indol-3-yl)methyl)indolin-2-one (111). The compound was synthesized using **107** (5 mmol) and was isolated as a yellow solid (96 % yield). ¹H NMR (500 MHz, DMSO-*d*₆) δ 11.13 – 10.52 (m, 1H), 10.21 (s, 1H), 7.26 (dd, *J* = 13.1, 3.6 Hz, 2H), 6.99 (d, *J* = 2.5 Hz, 1H), 6.95 (dd, *J* = 8.6, 2.8 Hz, 1H), 6.86 (dd, *J* = 18.5, 9.1, 2.7 Hz, 2H), 6.63 (dd, *J* = 8.4, 4.4 Hz, 1H), 3.79 (t, *J* = 5.8

Hz, 1H), 3.37 (dd, $J = 14.6, 5.0$ Hz, 1H), 3.16 (dd, $J = 14.6, 6.6$ Hz, 1H). ^{13}C NMR (126 MHz, DMSO- d_6) δ 178.75, 158.69, 157.70, 156.82, 155.87, 139.16, 132.63, 125.95, 113.78, 113.60, 112.38, 112.27, 112.19, 109.60, 109.53, 109.18, 108.98, 103.56, 103.37, 46.72, 24.91. LC-MS (m/z): positive mode 299 $[\text{M}+\text{H}]^{1+}$. Purity by HPLC UV (254 nm)-ESI-MS: 98 %. Mp: 154–156 °C.

5-Fluoro-3-((5-methoxy-1H-indol-3-yl)methyl)indolin-2-one (112). The compound was synthesized using **108** (5 mmol) and was isolated as a brown solid (91 % yield). ^1H NMR (500 MHz, DMSO- d_6) δ 10.56 (d, $J = 2.2$ Hz, 1H), 10.20 (s, 1H), 7.15 (d, $J = 8.8$ Hz, 1H), 7.00 (d, $J = 2.4$ Hz, 1H), 6.93 – 6.81 (m, 3H), 6.67 – 6.58 (m, 2H), 3.83 – 3.74 (m, 1H), 3.71 (s, 3H), 3.41 – 3.32 (m, 1H), 3.12 (dd, $J = 14.6, 7.1$ Hz, 1H). $^{13}\text{C}_{\text{apt}}$ NMR (126 MHz, DMSO- d_6) δ 178.75, 158.62, 156.75, 153.06, 139.17, 131.17, 127.64, 124.50, 113.73, 113.55, 112.45, 112.26, 111.96, 111.25, 110.04, 109.56, 109.49, 100.62, 55.38, 46.70, 25.21. LC-MS (m/z): positive mode 311 $[\text{M}+\text{H}]^{1+}$. Purity by HPLC UV (254 nm)-ESI-MS: >98 %. Mp: 162–164 °C.

3-((1H-Indol-5-yl)methyl)indolin-2-one (113). The compound was synthesized using **109** (5 mmol) and was isolated as a brown (95 % yield). ^1H NMR (500 MHz, DMSO- d_6) δ 10.91 (s, 1H), 10.22 (s, 1H), 7.31 – 7.22 (m, 2H), 7.20 (d, $J = 8.2$ Hz, 1H), 7.05 (dd, $J = 7.2, 2.4$ Hz, 1H), 6.88 (dd, $J = 8.2, 1.8$ Hz, 1H), 6.78 (d, $J = 6.6$ Hz, 2H), 6.68 (d, $J = 7.7$ Hz, 1H), 6.28 (t, $J = 2.5$ Hz, 1H), 3.76 (dd, $J = 8.0, 4.9$ Hz, 1H), 3.38 (dd, $J = 13.9, 5.0$ Hz, 1H), 2.96 (dd, $J = 13.8, 8.0$ Hz, 1H). $^{13}\text{C}_{\text{apt}}$ NMR (126 MHz, DMSO- d_6) δ 178.44, 142.77, 134.81, 129.46, 128.23, 127.68, 127.50, 125.37, 124.51, 122.71, 120.90, 120.53, 110.98, 109.13, 100.88, 47.25, 35.75. LC-MS (m/z): positive mode 263 $[\text{M}+\text{H}]^{1+}$. Purity by HPLC UV (254 nm)-ESI-MS: 99 %. Mp: 182–184 °C.

Biological assays

The recombinant CHO cell line expressing the human GPR84 (CHO-hGPR84 cells) with a β -galactosidase fragment and arrestin containing the complementary fragment of the enzyme for

performing β -arrestin recruitment assays based on enzyme complementation technology with a luminescent readout (Pathhunter[®]) was purchased from DiscoverX (Fremont, CA). This cell line was used for the β -arrestin recruitment assays as well as for cAMP accumulation assays. The CHO-hGPR84 cells were cultured in F12 medium supplemented with 10 % FCS, 100 units/mL penicillin G, 100 μ g/mL streptomycin, 800 μ g/mL G 418, 300 μ g/mL hygromycin B, and 1 % ultraglutamin (Invitrogen, Carlsbad, CA or Sigma-Aldrich, St. Louis, MO). Stock solutions of compounds including forskolin were prepared in DMSO. The final DMSO concentration in the assays did not exceed 1%. Data analysis was performed with GraphPad Prism (Version 6.02). Concentration-response data were fitted by non-linear regression to estimate EC₅₀ values (Prism 6.02). Statistical analysis was performed using GraphPad Prism 6.02. Differences between means were calculated using two-tailed Student's t test and a p-value of < 0.05 was considered statistically significant. The cooperativity factor α and the equilibrium dissociation constant K_b for allosteric modulation were calculated by fitting the data to the "allosteric EC₅₀ shift" equation (Prism 6.02).

GPR84 cAMP accumulation assays

CHO-hGPR84 cells were cultured on 24-well plates for 24 h. The culture medium was removed and cells were incubated with Hanks Balanced Salt Solution (HBSS) buffer (pH 7.4) at 37°C in presence of the cAMP phosphodiesterase inhibitor RO-20-1724 (final concentration of 40 μ M). Cells were then stimulated by addition of forskolin (10 μ M) in the absence (control) or presence of test compounds for 15 min. After removal of the buffer, cells were lysed by the addition of a hot (90 °C) lysis solution containing 4 mM EDTA, and 0.01 % Triton X-100 in water. AMP levels in the supernatant were quantified by a radiometric assay using a cAMP binding protein prepared from bovine adrenal medulla and [³H]cAMP (Perkin-Elmer, Rodgau, Germany) as described previously.⁹⁰ The forskolin-induced increase in cAMP concentration in the presence of agonists was expressed as percentage of the response to forskolin in the absence of agonists (% of control). Three independent experiments were performed, each in duplicates.

GPR84 β -arrestin recruitment assays

β -Arrestin assays were performed as previously described.⁹¹ CHO-hGPR84 cells (20,000 per well) in 90 μ L of Cell Plating 2 Reagent (DiscoverX[®]) were seeded into 96-well plates (Thermo Scientific, Waltham, MA). Compound dilutions (in DMSO, 10 μ L per well) were added to the cells. The final DMSO concentration did not exceed 1 %. After 90 min of incubation, 50 μ L of detection reagent (DiscoverX[®]) per well were added. After 60 min of incubation at rt the luminescence was measured using an NXT plate reader (Perkin-Elmer, Rodgau, Germany). Three to five independent experiments were performed, each in duplicates.

FFAR4 β -arrestin recruitment assays

A parental CHO β -arrestin cell line and the corresponding expression vectors were purchased from DiscoverX (Freemont, CA). After subcloning of the human FFAR4 (GPR120) cDNA sequence into a suitable expression vector, the parental cell line was transfected with the DNA construct by lipofection. Using these cells recombinantly expressing the human FFAR4 the assay was essentially performed as previously described.⁹¹ In brief, on the day before the assay the cells were seeded into a white 96-well plate at a density of 30,000 cells per well. Approximately four hours prior to the assay the medium was exchanged for 90 μ L of serum-free F12 medium per well. Test compounds were diluted in DMSO followed by a subsequent dilution step in serum-free medium (resulting in a final concentration of 1% DMSO in the assay). In antagonist assays test compound dilutions (5 μ L per well) were added 30 min before the addition of the reference agonist 4-[(4-fluoro-4'-methyl[1,1'-biphenyl]-2-yl)methoxy]-benzenepropanoic acid (TUG-891, 5 μ L per well, final concentration 4 μ M \approx EC₈₀). In agonist assays 10 μ L of test compound dilutions were added. After 90 min in the presence of an agonist, 50 μ L of a detection reagent was added to each well. After an incubation of 60 min at rt in the dark, luminescence in each well was measured using an NXT plate reader (Perkin-Elmer, Meriden, CT). All compounds were tested at a final concentration of 10 μ M. Test results were normalized to values obtained by

determining the background and the signal induced by 30 μ M and 4 μ M of TUG-891 in agonist and antagonist assays, respectively. Three to four independent experiments were performed in duplicates.

FFAR1 calcium mobilization assay

To generate a cell line for calcium mobilization assays the cDNA sequence of FFAR1 (GPR40) was inserted into the retroviral plasmid pLXSN. The retroviral transfection of 1321N1 astrocytoma cells was performed as previously described.⁹⁰ On the day before the assay the cells recombinantly expressing FFAR1 were seeded into 96-well plates (black, clear bottom) at a density of 50,000 cells per well. The cells were cultured in DMEM medium supplemented with 10 % FCS, 100 units/mL penicillin G, 100 μ g/mL streptomycin and 800 μ g/mL G418. On the day of the assay the medium was exchanged for 40 μ l of a HBSS buffer solution containing 3 μ M of the calcium dye Fluo-4-AM (Life Technology, Darmstadt, Germany) and 0.06 % Pluronic F-127. After 60 min of incubation at rt in the dark the dye solution was exchanged for 190 μ l and 189 μ l of HBSS buffer, in agonist and antagonist assays, respectively. Using a FlexStation[®] 3 plate reader (Molecular Devices, Sunnyvale, CA) 10 μ l of test compound solution were added to each well. In antagonist assays cells were preincubated for 30 min with test compound solutions (1 μ l per well) before the reference agonist 3-(4-(*o*-tolylethynyl)phenyl)propanoic acid (TUG-424) was added (10 μ l per well, final concentration: 1 μ M \approx EC₈₀). The final DMSO concentration did not exceed 1 %. Fluorescence was measured at 520 nm (excitation 485 nm) for 90 intervals of 1.2 s each. All compounds were tested at a final concentration of 10 μ M. Signals induced by the test compounds were normalized to the signals induced by 1 μ M and 10 μ M of TUG-424, in antagonist and agonist assays, respectively. Three to four independent experiments were performed in duplicates.

Arylhydrocarbon receptor (AhR) activation

HepG2 cells (3×10^5 cells/ml) were stimulated for 18 h with 5 μ M or 20 μ M of diindolylmethane, **38**, **57**, or left untreated. 3-Methylcholanthrene (3MC, 10 μ M) was used as a positive control. RNA was extracted using the Quick RNATM Mini prep kit (Zymo Research, Irvine, CA, U.S.A.) according to the manufacturer's instructions. First-strand cDNA was synthesized from 500 ng of total RNA using oligo(dT)₁₂₋₁₈ primers and RevertAid reverse transcriptase (Thermo Fischer Scientific, Schwerte, Germany). Real time PCR was performed in a CFX96 Real time System (Biorad, Hercules, CA, USA) using absolute SYBR-green ROX master mix (Thermo Fisher Scientific). *Cyp1A1* expression levels were normalized to *gapdh* and were displayed as fold-change relative to untreated samples used as the calibrator (set to 1). Primers for *cyp1A1* and *gapdh* were: *cyp1A1*-fwd: 5'-cag gta tgt ggt ggt atc agg-3' and *cyp1A1*-rev: 5'-ggg agg tag cga aga ata gg-3'; *gapdh*-fwd: agc cac atc gct cag aca c and *gapdh*-rev: gcc caa tac gac caa atc c-3'. Three independent experiments were performed.

Determination of stability

Stability of selected compounds in acidic, neutral and basic solutions was measured using LC-MS analysis.⁸⁹ The artificial gastric acid was prepared as previously described.^{92,93} Pepsin (3.2 g), NaCl (2.0 g) and HCl (1 M, 80 mL) were mixed with pure water to obtain 1000 mL (pH 1.2), and the resulting solution was stored at 4 °C. Stock solutions (2.5 mM) of **1**, **38**, and **52** were prepared in a mixture of methanol/acetonitrile (1:1) and 40 μ L of stock solution was added to 960 μ L of water or 0.01% aqueous ammonia solution (pH 9), or 1 mM sodium hydroxide solution (pH 11) or artificial gastric acid yielding a final compound concentration of 100 μ M. The solutions were incubated at 37 °C for up to 24 h and subsequently analyzed at regular time intervals. Mass spectra were recorded on a microOTOF-Q mass spectrometer (Bruker) with an ESI-source coupled with an HPLC Dionex Ultimate 3000 (Thermo Scientific) using an EC50/2 Nucleodur C18 Gravity 3 μ m column (Macherey-Nagel). The column temperature was 25 °C. The HPLC separation started with 90 % water containing 2 mM ammonium acetate and 10 % acetonitrile. A gradient started after 1 min to 100 % acetonitrile within 9 min. The

column was flushed with 100 % acetonitrile for an additional period of 5 min. Sample solution (5 μ L) was injected at a flow rate of 0.3 mL/min. Positive full scan MS was observed from 50-1000 m/z.

ASSOCIATED CONTENT

Supporting Information

Melting points and purities of GPR84 agonists; potency of GPR84 agonists at the human fatty acid receptors FFAR1 and FFAR4 and the human GPR35; evaluation of selected arylhydrocarbon receptor ligands at GPR84 in cAMP assays; analysis of compound stability; ^1H , ^{13}C / $^{13}\text{C}_{\text{apt}}$ -NMR spectra of compounds **1**, **34**, **35**, **38**, **51-57**, **93** and **95**; molecular string formulae.

AUTHOR INFORMATION

Corresponding Author

*Dr. Christa E. Müller

Pharmazeutisches Institut

Pharmazeutische Chemie I

An der Immenburg 4, D-53121 Bonn, Germany

Phone: +49-228-73-2301

Fax: +49-228-73-2567

E-mail: christa.mueller@uni-bonn.de

ACKNOWLEDGMENTS

T.P. is grateful to the Alexander von Humboldt (AvH) foundation and to Bayer Pharma for supporting a postdoctoral fellowship. G.B. thanks the CAPES Foundation and the Ministry of Education of Brazil for supporting an internship. I.F. is a member of the DFG-funded Cluster of Excellence ImmunoSensation.

We thank Marion Schneider for LCMS analyses, Sabine Terhart-Krabbe and Annette Reiner for NMR studies and Daniel Müller for performing some of the β -arrestin assays.

ABBREVIATIONS USED

GPCR, G protein-coupled receptor; cAMP, cyclic adenosine monophosphate; GPR, G protein-coupled receptor; FFA/R, free fatty acid/receptor; M/L/SCFA, medium/long/short chain fatty acid; GLP-1, glucagon like peptide-1; PTX, pertussis toxin; Th, T helper; TB, tuberculosis; TNF, tumor necrosis factor; TM, transmembrane; CHO, Chinese hamster ovary; SAR, structure-activity relationship; DIM, Diindolylmethane; SDS, sodium dodecylsulfate; CTAB, *N*-acetyl-*N,N,N*-trimethylammonium bromide; MW, microwave; DCE, dichloroethane; DMSO, dimethyl sulfoxide; TFAA, trifluoroacetic acid; NMR, nuclear magnetic resonance; HPLC, high performance liquid chromatography; ESI, electrospray ionization; EA, ethyl acetate; DCM, dichloromethane; TLC, thin layer chromatography; PE, petrolether; DMF, *N,N'*-dimethylformamide; THF, tetrahydrofuran.

References

- (1) Rask-Andersen, M.; Almen, M. S.; Schioth, H. B. Trends in the exploitation of novel drug targets. *Nat. Rev. Drug Discovery* **2011**, *10*, 579–590.
- (2) Chung, S.; Funakoshi, T.; Civelli, O. Orphan GPCR research. *Br. J. Pharmacol.* **2008**, *153 Suppl 1*, S339-346.
- (3) Briscoe, C. P.; Tadayyon, M.; Andrews, J. L.; Benson, W. G.; Chambers, J. K.; Eilert, M. M.; Ellis, C.; Elshourbagy, N. A.; Goetz, A. S.; Minnick, D. T.; Murdock, P. R.; Sauls, H. R. Jr.; Shabon, U.; Spinage, L. D.; Strum, J. C.; Szekeres, P. G.; Tan, K. B.; Way, J. M.; Ignar, D. M.; Wilson, S.; Muir, A.

- 1 I. The orphan G protein-coupled receptor GPR40 is activated by medium and long chain fatty acids. *J.*
2
3 *Biol. Chem.* **2003**, 278, 11303–11311.
- 4
5 (4) Brown, A. J.; Goldsworthy, S. M.; Barnes, A. A.; Eilert, M. M.; Tcheang, L.; Daniels, D.; Muir, A.
6
7 I.; Wigglesworth, M. J.; Kinghorn, I.; Fraser, N. J.; Pike, N. B.; Strum, J. C.; Steplewski, K. M.;
8
9 Murdock, P. R.; Holder, J. C.; Marshall, F. H.; Szekeres, P. G.; Wilson, S.; Ignar, D. M.; Foord, S. M.;
10
11 Wise, A.; Dowell, S. The Orphan G protein-coupled receptors GPR41 and GPR43 are activated by
12
13 propionate and other short chain carboxylic acids. *J. Biol. Chem.* **2003**, 278, 11312–11319.
- 14
15
16
17 (5) Hirasawa, A.; Tsumaya, K.; Awaji, T.; Katsuma, S.; Adachi, T.; Yamada, M.; Sugimoto, Y.;
18
19 Miyazaki, S.; Tsujimoto, G. Free fatty acids regulate gut incretin glucagon-like peptide-1 secretion
20
21 through GPR120. *Nat. Med.* **2005**, 11, 90–94.
- 22
23
24 (6) Itoh, Y.; Kawamata, Y.; Harada, M.; Kobayashi, M.; Fujii, R.; Fukusumi, S.; Ogi, K.; Hosoya, M.;
25
26 Tanaka, Y.; Uejima, H.; Tanaka, H.; Maruyama, M.; Satoh, R.; Okubo, S.; Kizawa, H.; Komatsu, H.;
27
28 Matsumura, F.; Noguchi, Y.; Shinohara, T.; Hinuma, S.; Fujisawa, Y.; Fujino, M. Free fatty acids
29
30 regulate insulin secretion from pancreatic beta cells through GPR40. *Nature* **2003**, 422, 173–176.
- 31
32
33 (7) Inoue, D.; Tsujimoto, G.; Kimura, I. Regulation of energy homeostasis by GPR41. *Front.*
34
35 *Endocrinol. (Lausanne)*. **2014**, 5, 81.
- 36
37
38 (8) Blad, C. C.; Tang, C.; Offermanns, S. G protein-coupled receptors for energy metabolites as new
39
40 therapeutic targets. *Nat. Rev. Drug Discovery* **2012**, 11, 603–619.
- 41
42
43 (9) Wang, J.; Wu, X.; Simonavicius, N.; Tian, H.; Ling, L. Medium-chain fatty acids as ligands for
44
45 orphan G protein-coupled receptor GPR84. *J. Biol. Chem.* **2006**, 281, 34457–34464.
- 46
47
48 (10) Bouchard, C.; Pagé, J.; Bédard, A.; Tremblay, P.; Vallières, L. G protein-coupled receptor 84, a
49
50 microglia-associated protein expressed in neuroinflammatory conditions. *Glia* **2007**, 55, 790–800.
- 51
52
53 (11) Oh, D. Y.; Talukdar, S.; Bae, E. J.; Imamura, T.; Morinaga, H.; Fan, W.; Li, P.; Lu, W. J.; Watkins,
54
55 S. M.; Olefsky, J. M. GPR120 is an ω -3 fatty acid receptor mediating potent anti-inflammatory and
56
57 insulin-sensitizing effects. *Cell* **2010**, 142, 687–698.
- 58
59
60

- (12) Kotarsky, K.; Nilsson, N. E.; Flodgren, E.; Owman, C.; Olde, B. A human cell surface receptor activated by free fatty acids and thiazolidinedione drugs. *Biochem. Biophys. Res. Commun.* **2003**, *301*, 406–410.
- (13) Le Poul, E.; Loison, C.; Struyf, S.; Springael, J. Y.; Lannoy, V.; Decobecq, M-E.; Brezillon, S.; Dupriez, V.; Vassart, G.; Damme, J. V.; Parmentier, M.; Detheux, M. Functional characterization of human receptors for short chain fatty acids and their role in polymorphonuclear cell activation. *J. Biol. Chem.* **2003**, *278*, 25481–25489.
- (14) Nilsson, N. E.; Kotarsky, K.; Owman, C.; Olde, B. Identification of a free fatty acid receptor, FFA2R, expressed on leukocytes and activated by short-chain fatty acids. *Biochem. Biophys. Res. Commun.* **2003**, *303*, 1047–1052.
- (15) Cornish, J.; MacGibbon, A.; Lin, J. M.; Watson, M.; Callon, K. E.; Tong, P. C.; Dunford, J. E.; van der Does, Y.; Williams, G. A.; Grey, A. B.; Naot, D.; Reid, I. R. Modulation of osteoclastogenesis by fatty acids. *Endocrinology* **2008**, *149*, 5688–5695.
- (16) Wauquier, F.; Philippe, C.; Léotoing, L.; Mercier, S.; Davicco, M. J.; Lebecque, P.; Guicheux, J.; Pilet, P.; Miot-Noirault, E.; Poitout, V.; Alquier, T.; Coxam, V.; Wittrant, Y. The free fatty acid receptor G protein-coupled receptor 40 (GPR40) protects from bone loss through inhibition of osteoclast differentiation. *J. Biol. Chem.* **2013**, *288*, 6542–6551.
- (17) Cartoni, C.; Yasumatsu, K.; Ohkuri, T.; Shigemura, N.; Yoshida, R.; Godinot, N.; le Coutre, J.; Ninomiya, Y.; Damak, S. Taste preference for fatty acids is mediated by GPR40 and GPR120. *J. Neurosci.* **2010**, *30*, 8376–8382.
- (18) Hong, Y. H.; Nishimura, Y.; Hishikawa, D.; Tsuzuki, H.; Miyahara, H.; Gotoh, C.; Choi, K. C.; Feng, D. D.; Chen, C.; Lee, H. G.; Katoh, K.; Roh, S. G.; Sasaki, S. Acetate and propionate short chain fatty acids stimulate adipogenesis via GPCR43. *Endocrinology* **2005**, *146*, 5092–5099.
- (19) Nøhr, M. K.; Pedersen, M. H.; Gille, A.; Egerod, K. L.; Engelstoft, M. S.; Husted, A. S.; Sichlau, R. M.; Grunddal, K. V.; Poulsen, S. S.; Han, S.; Jones, R. M.; Offermanns, S.; Schwartz, T. W.

- GPR41/FFAR3 and GPR43/FFAR2 as cosensors for short-chain fatty acids in enteroendocrine cells vs FFAR3 in enteric neurons and FFAR2 in enteric leukocytes. *Endocrinology* **2013**, *154*, 3552-3564.
- (20) Wittenberger, T.; Schaller, H. C.; Hellebrand, S. An expressed sequence tag (EST) data mining strategy succeeding in the discovery of new G-protein coupled receptors. *J. Mol. Biol.* **2001**, *307*, 799-813.
- (21) Yousefi, S.; Cooper, P. R.; Potter, S. L.; Mueck, B.; Jarai, G. Cloning and expression analysis of a novel G protein-coupled receptor selectively expressed on granulocytes. *J. Leukoc. Biol.* **2001**, *69*, 1045-1052.
- (22) Lattin, J. E.; Schroder, K.; Su, A. I.; Walker, J. R.; Zhang, J.; Wiltshire, T.; Saijo, K.; Glass, C. K.; Hume, D. A.; Kellie, S.; Sweet, M. J. Expression analysis of G protein-coupled receptors in mouse macrophages. *Immunome Res.* **2008**, *4*, 1-13.
- (23) Dietrich, P. A.; Yang, C.; Leung, H. H. L.; Lynch, J. R.; Gonzales, E.; Liu, B.; Haber, M.; Norris, M. D.; Wang, J. L.; Wang, J. Y. GPR84 sustains aberrant beta-catenin signaling in leukemic stem cells for maintenance of MLL leukemogenesis. *Blood* **2014**, *124*, 3284-3294.
- (24) Nagasaki, H.; Kondo, T.; Fuchigami, M.; Hashimoto, H.; Sugimura, Y.; Ozaki, N.; Arima, H.; Ota, A.; Oiso, Y.; Hamada, Y. Inflammatory changes in adipose tissue enhance expression of GPR84, a medium-chain fatty acid receptor: TNF α enhances GPR84 expression in adipocytes. *FEBS Letters*, **2012**, *586*, 368-372.
- (25) Audoy-Remus, J.; Bozoyan, L.; Dumas, A.; Filali, M.; Cynthia, L.; Lacroix, S.; Rivest, S.; Tremblay, M. E.; Vallieres, L. GPR84 deficiency reduces microgliosis, but accelerates dendritic degeneration and cognitive decline in a mouse model of Alzheimer's disease. *Brain Behav. Immun.* **2015**, *46*, 112-120.
- (26) Nicol, L. S.; Dawes, J. M.; La Russa, F.; Didangelos, A.; Clark, A. K.; Gentry, C.; Grist, J.; Davies, J. B.; Malcangio, M.; McMahon, S. B. The role of G-protein receptor 84 in experimental neuropathic pain. *J. Neurosci.* **2015**, *35*, 8959-8969.

- (27) Abdel-Aziz, H.; Schneider, M.; Neuhuber, W.; Kassem, A. M.; Khailah, S.; Muller, J.; Gamaleldeen, H.; Khairy, A.; Khayyal, M. T.; Shcherbakova, A.; Efferth, T.; Ulrich-Merzenich, G. GPR84 and TREM-1 signaling contribute to the pathogenesis of reflux esophagitis. *Mol. Med.* **2015**, *21*, 1011-1024.
- (28) Dupont, S.; Arijs, I.; Blanque, R.; Laukens, D.; Nys, K.; Ceccotti, M. C.; Merciris, D.; De Vos, S.; Mate, O.; Parent, I.; De Vriendt, V.; Labeguere, F.; Galien, R.; Devos, M.; Rutgeerts, P.; Vandeghinste, N.; Vermeire, S.; Brys, R. GPR84 inhibition as a novel therapeutic approach in IBD: mechanistic and translational studies. *J. Crohns Colitis* **2015**, *9*, S92–S93.
- (29) Suzuki, M.; Takaishi, S.; Nagasaki, M.; Onozawa, Y.; Iino, I.; Maeda, H.; Komai, T.; Oda, T. Medium-chain fatty acid-sensing receptor, GPR84, is a proinflammatory receptor. *J. Biol. Chem.* **2013**, *288*, 10684-10691.
- (30) Christiansen, E.; Watterson, K. R.; Stocker, C. J.; Sokol, E.; Jenkins, L.; Simon, K.; Grundmann, M.; Petersen, R. K.; Wargent, E. T.; Hudson, B. D.; Kostenis, E.; Ejlsing, C. S.; Cawthorne, M. A.; Milligan, G.; Ulven, T. Activity of dietary fatty acids on FFA1 and FFA4 and characterisation of pinolenic acid as a dual FFA1/FFA4 agonist with potential effect against metabolic diseases. *Br. J. Nutr.* **2015**, *113*, 1677-1688.
- (31) Offermanns, S. Free fatty acid (FFA) and hydroxy carboxylic acid (HCA) receptors. Free fatty acid (FFA) and hydroxy carboxylic acid (HCA) receptors. *Annu. Rev. Pharmacol. Toxicol.* **2014**, *54*, 407-434.
- (32) Zhang, Q.; Yang, H.; Li, J.; Xie, X. Discovery and characterization of a novel small molecule agonist for medium chain free fatty acid receptor GPR84. *J. Pharmacol. Exp. Ther.* **2016**, *357*, 337-344.
- (33) Liu, Y.; Zhang, Q.; Chen, L. H.; Yang, H.; Lu, W.; Xie, X.; Nan, F. J. Design and synthesis of 2-alkylpyrimidine-4,6-diol and 6-alkylpyridine-2,4-diol as potent GPR84 agonists. *ACS Med. Chem. Lett.* **2016**, *7*, 579–583.

- (34) Hakak, Y.; Unett, D. J.; Gatlin, J.; Liaw, C. W. Human G protein-coupled receptor and modulators thereof for the treatment of atherosclerosis and atherosclerotic disease and for the treatment of conditions related to MCP-1 expression. WO2007027661 A3, April 26, 2007.
- (35) Krishnaswamy, M.; Purushothaman, K. K. Antifertility properties of Embelia ribes: (embelin). *Indian J. Exp. Biol.* **1980**, *18*, 1359-1360.
- (36) Chitra, M.; Sukumar, E.; Suja, V.; Devi, C. S. Antitumor, anti-inflammatory and analgesic property of embelin, a plant product. *Chemotherapy* **1994**, *40*, 109-113.
- (37) Chitra, M.; Devi, C. S.; Sukumar, E. Antibacterial activity of embelin. *Fitoterapia* **2003**, *74*, 401-403.
- (38) Nikolovska-Coleska, Z.; Xu, L.; Hu, Z.; Tomita, Y.; Li, P.; Roller, P. P.; Wang, R.; Fang, X.; Guo, R.; Zhang, M.; Lippman, M. E.; Yang, D.; Wang, S. Discovery of embelin as a cell-permeable, small-molecular weight inhibitor of XIAP through structure-based computational screening of a traditional herbal medicine three-dimensional structure database. *J. Med. Chem.* **2004**, *47*, 2430-2440.
- (39) Joshi, R.; Kamat, J. P.; Mukherjee, T. Free radical scavenging reactions and antioxidant activity of embelin: biochemical and pulse radiolytic studies. *Chem. Biol. Interact.* **2007**, *167*, 125-134.
- (40) Takeda, S.; Yamamoto, A.; Okada, T.; Matsumura, E.; Nose, E.; Kogure, K.; Kojima, S.; Haga, T. Identification of surrogate ligands for orphan G protein-coupled receptors. *Life Sci.* **2003**, *74*, 367-377.
- (41) Nikaido, Y.; Koyama, Y.; Yoshikawa, Y.; Furuya, T.; Takeda, S. Mutation analysis and molecular modeling for the investigation of ligand-binding modes of GPR84. *J. Biochem.* **2015**, *157*, 311-320.
- (42) Wang, T. T.; Schoene, N. W.; Milner, J. A.; Kim, Y. S. Broccoli-derived phytochemicals indole-3-carbinol and 3,3'-diindolylmethane exerts concentration-dependent pleiotropic effects on prostate cancer cells: comparison with other cancer preventive phytochemicals. *Mol. Carcinog.* **2012**, *51*, 244-256.
- (43) Yin, X. F.; Chen, J.; Mao, W.; Wang, Y. H.; Chen, M. H. A selective aryl hydrocarbon receptor modulator 3,3'-diindolylmethane inhibits gastric cancer cell growth. *J. Exp. Clin. Cancer. Res.* **2012**, *31*, 31-46.

- (44) Marques, M.; Laflamme, L.; Benassou, I.; Cissokho, C.; Guillemette, B.; Gaudreau, L. Low levels of 3,3'-diindolylmethane activate estrogen receptor α and induce proliferation of breast cancer cells in the absence of estradiol. *BMC Cancer* **2014**, *14*, 524.
- (45) Seo, S. G.; Shin, S. H.; Min, S.; Kwon, J. Y.; Kim, K. H.; Lee, K. W.; Lee, H. J. 3,3'-Diindolylmethane inhibits adipogenesis of 3T3-L1 preadipocytes by proteosomal degradation of cyclin D1. *FASEB J.* **2011**, *25*, Supplement 581.15
- 46 (a) Fares, F. The anti-carcinogenic effect of indole-3-carbinol and 3, 3'-diindolylmethane and their mechanism of action. *Med. Chem.* **2014**, *SI*, 002, 1-8. (b) Kiselev, V. I.; Drukh, V. M.; Muyzhnek, E. L.; Kuznetsov, I. N.; Pchelintseva, O. I.; Paltsev, M. A. Preclinical antitumor activity of the diindolylmethane formulation in xenograft mouse model of prostate cancer. *Exp. Oncol.* **2014**, *36*, 90-93. (c) Firestone, G. L.; Bjeldanes, L. F. Indole-3-carbinol and 3-3'-diindolylmethane antiproliferative signaling pathways control cell-cycle gene transcription in human breast cancer cells by regulating promoter-Sp1 transcription factor interactions. *J. Nutr.* **2003**, *133* (Suppl), 2448S-2455S.
- (47) Zhang, M. Z.; Chen, Q.; Yang, G. F. A review on recent developments of indole-containing antiviral agents. *Eur. J. Med. Chem.* **2015**, *89*, 421-441.
- (48) Hemalathaa, K.; Madhumitha, G.; Mohana Roopan, S. Indole as a core anti-inflammatory agent- a mini review. *Che. Sci. Rev. Lett.* **2013**, *2*, 287-292.
- (49) El Sayed, M. T.; Hamdy, M. A.; Osman, D. A.; Ahmed, K. M. Indoles as anti-cancer agents. *Adv. Mod. Oncol. Res.* **2015**, *1*, 20-35.
- (50) Gregorovich, B. V.; Liang, K.; Clugston, M.; Macdonald, S. Reductive C-alkylation. *Can. J. Chem.* **1968**, *46*, 3291-3300.
- (51) Roomi, M.; Macdonald, S. Cyclizative condensation. I. 2- Methylindole with acetone and methyl ethyl ketone. *Can. J. Chem.* **1970**, *48*, 139-143.
- (52) Auria, M. Photochemical synthesis of diindolylmethanes. *Tetrahedron* **1991**, *47*, 9225-9230.
- (53) Chatterjee, A.; Manna, S.; Benerji, J.; Pascard, C.; Prange, T.; Shoolery, J. Lewis-acid-induced electrophilic substitution in indoles with acetone. Part 2. *J. Chem. Soc. Perkin Trans.* **1980**, *1*, 553-555.

- (54) Noland, W. E.; Venkiteswaran, M. R.; Richards, C. G. Cyclizative condensations. I. 2-Methylindole with acetone and methyl ethyl ketone. *J. Org. Chem.* **1961**, *26*, 4241–4248.
- (55) Chen, D. P.; Yu, L. B.; Wang, P. G. Lewis acid-catalyzed reactions in protic media. Lanthanide-catalyzed reactions of indoles with aldehydes or ketones. *Tetrahedron Lett.* **1996**, *37*, 4467–4470.
- (56) Nagarajan, R.; Perumal, P. T. InCl₃ and In(OTf)₃ catalyzed reactions: Synthesis of 3-acetyl indoles, diindolylmethane and indolylquinoline derivatives. *Tetrahedron* **2002**, *58*, 1229–1232.
- (57) Mi, X. L.; Luo, S. Z.; He, J. Q.; Chen, J. P. Dy(OTf)₃ in ionic liquid: An efficient catalytic system for reactions of indole with aldehydes/ketones or imines. *Tetrahedron Lett.* **2004**, *45*, 4567–4570.
- (58) Ji, S. J.; Wang, S. Y.; Zhang, Y.; Loh, T. T. Facile synthesis of bis(indolyl)methanes using catalytic amount of iodine at room temperature under solvent-free conditions. *Tetrahedron* **2004**, *60*, 2051–2055.
- (59) Mallik, A. K.; Pal, R.; Guha, C.; Mallik, H. A convenient, eco-friendly, and efficient method for synthesis of bis(3-indolyl)methanes on water. *Green Chem. Lett. Rev.* **2012**, *5*, 321–327.
- (60) Deb, M. L.; Bhuyan, P. J. An efficient and clean synthesis of bis(indolyl)methanes in a protic solvent at room temperature. *Tetrahedron Lett.* **2006**, *47*, 1441–1443.
- (61) Ghorbani-Vaghei, R.; Veisi, H.; Keypour, H.; Dehghani-Firouzabadi, A. A. A practical and efficient synthesis of bis(indolyl)methanes in water, and synthesis of di-, tri-, and tetra(bis-indolyl)methanes under thermal conditions catalyzed by oxalic acid dihydrate. *Mol. Divers.* **2010**, *14*, 87–96.
- (62) Ji, S. J.; Zhou, M. F.; Gu, D. G.; Jiang, Z. Q.; Loh, T. P. Efficient Fe^{III}-catalyzed synthesis of bis(indolyl)methanes in ionic liquids. *Eur. J. Org. Chem.* **2004**, *7*, 1584–1587.
- (63) Yadav, J. S.; Reddy, B. V. S.; Sunita, S. Efficient and eco-friendly process for the synthesis of bis(1H-indol-3-yl)methanes using ionic liquids. *Adv. Synth. Catal.* **2003**, *345*, 349–352.
- (64) Babu, G.; Sridhar, N.; Perumal, P. T. A convenient method of synthesis of bis-indolylmethanes: indium trichloride catalyzed reactions of indole with aldehydes and schiff's bases. *Synth. Commun.* **2000**, *30*, 1609–1614.

- (65) Koshima, H.; Matsuoka, W. N-Bromosuccinimide catalyzed condensations of indoles with carbonyl compounds under solventfree conditions. *J. Heterocyc. Chem.* **2002**, *39*, 1089-1091.
- (66) Wang, L.; Han, J.; Tian, H.; Sheng, J.; Fan, Z.; Tang, X. Rare earth perfluorooctanoate [RE(PFO)₃]-catalyzed condensation of indoles with carbonyl compounds. *Synlett.* **2005**, *2*, 337-339.
- (67) Sun, C.; Zou, X.; Li, F. Direct use of methanol as an alternative to formaldehyde for the synthesis of 3,3'-diindolylmethanes (3,3'-DIMs). *Chem. Eur. J.* **2013**, *19*, 14030-14033.
- (68) Maciejewskaa, D.; Rasztawickaa, M.; Wolskab, I.; Anuszewskac, E.; Gruberc, B. Novel 3,3'-diindolylmethane derivatives: synthesis and cytotoxicity, structural characterization in solid state. *Euro. J. Med. Chem.* **2009**, *44*, 4136-4147.
- (69) Maciejewskaa, D.; Wolskab, I.; Niemyjskaa, M.; Żeroa, P. Structure in solid state of 3,3'-diindolylmethane derivatives, potent cytotoxic agents against human tumor cells, followed X-ray diffraction and ¹³C CP/MAS NMR analyses. *J. Mol. Struct.* **2005**, *753*, 53-60.
- (70) Fei, H.; Yu, J.; Jiang, Y.; Guoa, H.; Cheng, J. The ammonium-promoted formylation of indoles by DMSO and H₂O: *Org. Biomol. Chem.* **2013**, *11*, 7092-7095.
- (71) (a) Manabe, K.; Mori, Y.; Kobayashi, S. Three-component carbon-carbon bondforming reactions catalyzed by a Bronsted acid-surfactant-combined catalyst in water. *Tetrahedron* **2001**, *57*, 2537-2544.
- (b) Jin, T. S.; Zhang, J. S.; Xiao, J. C.; Wang, A. Q.; Li, T. S. Clean synthesis of 1,8-dioxooctahydroxanthene derivatives catalyzed by p-dodecylbenzenesulfonic acid in aqueous media. *Synlett* **2004**, *5*, 866-870. (c) Jin, T. S.; Zhang, J. S.; Guo, T. T.; Wang, A. Q. One-pot clean synthesis of 1,8- dioxo decahydroacridines catalyzed by p-dodecylbenzenesulfonic acid in aqueous media. *Synthesis* **2004**, *12*, 2001-2005. (d) Jin, T. S.; Zhang, J. S.; Wang, A. Q.; Li, T. S. Ultrasound-assisted synthesis of 1,8- dioxo-octahydroxanthene derivatives catalyzed by p-dodecylbenzenesulfonic acid in aqueous media, *Ultrason. Sonochem.* **2006**, *13*, 220-224.
- (72) Abe, T.; Nakamura, S.; Yanada, R.; Choshi, T.; Hibino, S.; Ishikura, M. One-pot construction of 3,3'-diindolylmethanes through Bartoli indole synthesis. *Org. Lett.* **2013**, *15*, 3622-3625.

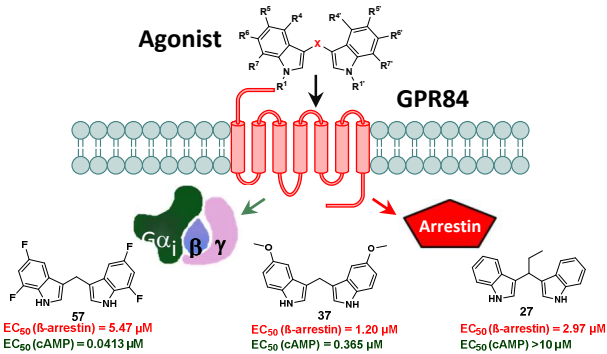
- (73) Armstrong, E. L.; Grover, H. K.; Kerr, M. A. Scandium triflate-catalyzed nucleophilic additions to indolylmethyl Meldrum's acid derivatives via a gramine-type fragmentation: synthesis of substituted indolemethanes. *J. Org. Chem.* **2013**, *78*, 10534-10540.
- (74) Xu, H-Y.; Zi, Y.; Xu, X-P.; Wang, S-Y.; Ji, S-J. TFA-catalyzed C-N bond activation of enamides with indoles: efficient synthesis of 3,3-diindolylpropanoates and other diindolylalkanes. *Tetrahedron* **2013**, *69*, 1600-1605.
- (75) Viola, A.; Ferrazzano, L.; Martelli, G.; Ancona, S.; Gentilucci, L.; Tolomelli, A. An improved microwave assisted protocol for Yonemitsu-type trimolecular condensation. *Tetrahedron* **2014**, *70*, 6781-6788.
- (76) Hasaninejad, A.; Zare, A.; Sharghi, H.; Khalifeh, R.; Reza, A.; Zare, M. PCl_5 as a mild and efficient catalyst for the synthesis of bis(indolyl)methanes and di-bis(indolyl)methanes. *Bull. Chem. Soc. Ethiop.* **2008**, *22*, 453-458.
- (77) Guchhait, S. K.; Kashyap, M.; Kamble, H. ZrCl_4 -mediated regio-and chemoselective Friedel-Crafts acylation of indole. *J. Org. Chem.* **2011**, *76*, 4753-4758.
- (78) Abe, T.; Ikeda, T.; Itoh, T.; Hatae, N.; Toyota, E.; Ishikura, M. One-pot access to 3,3'-diindolylmethanes through the intermolecular Pummerer reaction. *Heterocycles* **2014**, *88*, 187-191.
- (79) Thanigaimalai, P.; Lee, K. C.; Sharma, V. K.; Sharma, N.; Roh, E.; Kim, Y.; Jung, S. H. Identification of indoline-2-thione analogs as novel potent inhibitors of α -melanocyte stimulating hormone induced melanogenesis. *Chem. Pharm. Bull.* **2011**, *59*, 1285-1288.
- (80) Lee, H. J.; Lim, J. W.; Yu, J.; Kim, J. N. An expedient synthesis of 3-alkylideneoxindoles by $\text{Ti}(\text{OiPr})_4$ /pyridine-mediated Knoevenagel condensation. *Tetrahedron Lett.* **2014**, *55*, 1183-1187.
- (81) Shaveta.; Singh, P. Structural optimization of indole based compounds for highly promising anti-cancer activities: structure activity relationship studies and identification of lead molecules. *Eur. J. Med. Chem.* **2014**, *74*, 440-450.
- (82) Zou, H.; Zhang, L.; Ouyang, J.; Giulianotti, M. A.; Yu, Y. Synthesis and biological evaluation of 2-indolinone derivatives as potential antitumor agents. *Eur J. Med. Chem.* **2011**, *46*, 5970-5977.

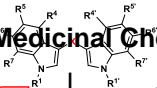
- (83) Tang, P. C.; Sun, L.; McMahon, G.; Miller, T. A.; Shirazian, S.; Wei, Chung C.; Harris, G. D.; Xiaoyuan, L.; Liang, C. Preparation of indolinones as protein kinase inhibitors. PCT Int. Appl. WO 2000056709 A1, September 28, 2000.
- (84) Southern, C.; Cook, J. M.; Neetoo-Isseljee, Z.; Taylor, D. L.; Kettleborough, C. A.; Merritt, A.; Bassoni, D. L.; Raab, W. J.; Quinn, E.; Wehrman, T. S.; Davenport, A. P.; Brown, A. J.; Green, A.; Wigglesworth, M. J.; Rees, S. Screening β -arrestin recruitment for the identification of natural ligands for orphan G protein-coupled receptors. *J. Biomol. Screen.* **2013**, *18*, 599-609.
- (85) <https://www.discoverx.com/Discoverx/media/ContentFiles/DataSheets/95-0158C2.pdf>, December 28, 2014.
- (86) Lee, T.; Schwandner, R.; Swaminath, G.; Weizmann, J.; Cardozo, M.; Greenberg, J.; Jaeckel, P.; Ge, H.; Wang, Y.; Jiao, X.; Liu, J.; Kayser, F.; Tian, H.; Li, Y. Identification and functional characterization of allosteric agonists for the G protein-coupled receptor FFA2. *Mol. Pharmacol.* **2008**, *74*, 1599-1609.
- (87) Müller, C. E.; Schiedel, A. C.; Baqi, Y. Allosteric modulators of rhodopsin-like G protein-coupled receptors: opportunities in drug development. *Pharmacol. Ther.* **2012**, *135*, 292-315.
- (88) Chen, I.; McDougal, A.; Wang, F.; Safe, S. Aryl hydrocarbon receptor-mediated antiestrogenic and antitumorigenic activity of diindolylmethane. *Carcinogenesis* **1998**, *19*, 1631-1639.
- (89) Brunschweiler, A.; Iqbal, J.; Umbach, F.; Scheiff, A. B.; Munkonda, M. N.; Sévigny, J.; Knowles, A. F.; Müller, C. E. Selective nucleoside triphosphate diphosphohydrolase-2 (NTPDase2) inhibitors: nucleotide mimetics derived from uridine-5'-carboxamide. *J. Med. Chem.* **2008**, *51*, 4518-4528.
- (90) Thimm, D.; Knospe, M.; Abdelrahman, A.; Moutinho, M.; Alsdorf, B. B. A.; Kügelgen, I. V.; Schiedel, A. C.; Müller, C. E. Characterization of new G protein-coupled adenine receptors in mouse and hamster. *Purinergic Signalling* **2013**, *9*, 415-426.
- (91) Thimm, D.; Funke, M.; Meyer, A.; Müller, C. E. 6-Bromo-8-(4- [3 H]methoxybenzamido)-4-oxo-4H-chromene-2-carboxylic acid: a powerful tool for studying orphan G protein-coupled receptor GPR35. *J. Med. Chem.* **2013**, *56*, 7084-7099.

(92) Yan, L.; Müller, C. E. Preparation, properties, reactions, and adenosine receptor affinities of sulfophenylxanthine nitrophenyl esters: toward the development of sulfonic acid prodrugs with peroral bioavailability. *J. Med. Chem.* **2004**, *47*, 1031-1043.

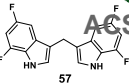
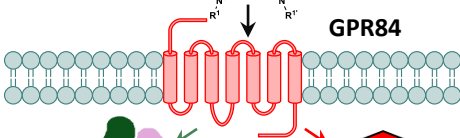
(93) Guven, K. C.; Ozaydin, F. Stability of sodium cyclamate in simulated gastric and intestinal media. *Pharmazie* **1981**, *36*, 297.

Table of Contents Graphic



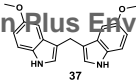


GPR84



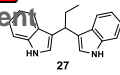
EC_{50} (β -arrestin) = 5.47 μ M

EC_{50} (cAMP) = 0.0413 μ M



EC_{50} (β -arrestin) = 1.20 μ M

EC_{50} (cAMP) = 0.365 μ M



EC_{50} (β -arrestin) = 2.97 μ M

EC_{50} (cAMP) >10 μ M